Rijksdienst voor Ondernemend Nederland

Openbaar eindrapport NexPas

Gegevens project

- Projectnummer: TEZ0214002
- Projecttitel: NexPas (“Passivated contacts in n-PASHA solar cells”)
- Penvoerder en medeaanvragers: Tempress Systems B.V., Yingli Energy (China) Co., Ltd., ECN, Universiteit Twente
- Projectperiode: 01-04-2015 t/m 30-09-2017
- Publicatiedatum openbaar rapport: 27-02-2018

Rijksdienst voor Ondernemend Nederland

Samenvatting van uitgangspunten, doelstelling en samenwerkende partijen

Eén manier om de kosten van elektriciteit opgewekt door PV systemen verder te verlagen, is het verhogen van het zonnecel- en modulerendement. De zeer efficiënte n-Pasha (bifacial n-type) zonnecel is ontwikkeld door ECN en Tempress Systems (beide uit Nederland) en andere partners. N-Pasha werd gedurende 2009/2010 in proefproductie gebracht door Yingli Green Energy, China, ECN en Tempress, en vervolgens sinds 2010 in productie genomen door Yingli. In 2014 werd een productielijn voor tweede generatie n-Pasha zonnecellen geïnstalleerd en gestart bij Mission Solar Energy in de VS. Inmiddels is een 3e generatie n-Pasha in ontwikkeling, en ook achterzijdecontact-varianten van n-Pasha zijn in pilot-productie getest. Al deze generaties n-Pasha hebben als gemeenschappelijke noemer dat productierijpheid en kosteneffectiviteit essentieel waren (en zijn) voor succes.

In de recente jaren is er een gestage toename van het celrendement gerealiseerd voor het n-Pasha zonnecelproces. Voor verdere verbetering van het rendement moet de rendementsbeperkende recombinatie bij de contacten in de zonnecel worden verminderd. Van gestapelde dunne films van een gedoteerde polysiliciumlaag op een zeer dunne diëlektrische laag is bewezen dat deze een zogenaamd gepassiveerd contact verschaffen aan het oppervlak van de silicium wafer, hetgeen resulteert in een zeer lage contactrecombinatie. Gepassiveerde contacten op basis van polysilicium (in het engels polysilicon, polySi, of kortweg poly) bestaan al lang in de micro-elektronica. Een dergelijk gepassiveerd contact is in 2014 door het Fraunhofer-instituut ISE gebruikt om een hoogrendements laboratorium-n-type zonnecel te creëren. Ook heeft SunPower Corporation gerapporteerd dat er gepassiveerde contacten worden gebruikt in hun nieuwste achterzijdecontact-zonnecellen.

Het doel van het NexPas project was om een industriële technologie voor polysilicium gepassiveerde contacten voor zonnecellen te ontwikkelen, en tevens een industrieel productieproces voor n-type zonnecellen te ontwikkelen met zo'n polysilicium gepassiveerd contact aan de achterzijde. Het doel van het gepassiveerde contact is om het celrendement aanzienlijk te verhogen. Rendemenstdoel van dit project was 22% celrendement op standaard industriële silicium *wafers* en met processen die relevant zijn voor toepassing in de PV industrie. Daarnaast moest het integrale celproces leiden tot lagere kosten in vergelijking met het huidige n-Pasha -celproces. In dit project werden de nieuwe processen om een gepassiveerd contact in n-Pasha cellen te implementeren ontwikkeld en getest op industriële toepasbaarheid, inclusief moduleproductie en betrouwbaarheidscontrole van die modules.

Het project richtte zich specifiek op massaproductiemethoden en -apparatuur. Voor wat betreft het gepassiveerde contact betekende dit ontwikkeling van processen voor de diëlektrische laag, de depositie van de polysiliciumlaag en dotering van die laag, met als doel het gepassiveerde contact goedkoop en betrouwbaar te kunnen produceren. Voor wat betreft de n-Pasha zonnecel betekende dit ontwikkeling van een integraal fabricageproces dat dit gepassiveerde contact op de achterkant van een n- Pasha-cel combineerde met conventionele voorzijde diffusie en voorzijde metaalcontacten. Dit omvatte nogal drastische aanpassing van het n-Pasha celproces op vele aspecten, en met name de metallisatie van het gepassiveerde contact moest in detail onderzocht worden.

De partners in dit project waren Tempress, Yingli Green Energy, ECN en de Universiteit Twente (UT). De coördinator Tempress ontwikkelde productie-apparatuur en, met ECN, processen voor het gepassiveerde contact. ECN ontwikkelde de integrale cel- en moduletechnologieën, en karakteriseerde de cellen in detail en bepaalde de verliesfactoren met behulp van speciale computersimulaties. Yingli droeg bij aan de ontwikkeling met productieprocessen uitgevoerd in haar R&D-lijnen, onderzocht de mogelijkheden om de technologieën in een massaproductieproces over te nemen, en onderzocht de stabiliteit van modules. UT leverde expertise op het gebied van polysilicium en metallisatie, alsmede karakterisering.

Zowel Tempress als ECN ondervinden belangstelling van meerdere industriële partijen voor de n-type celtechnologie en Tempress krijgt in het bijzonder veel belangstelling voor de technologie voor polysilicium gepassiveerde contacten. De resultaten van dit project versterken de marktpositie van Tempress in meerdere opzichten (voor n-type zonnecellen, voor polysilicium, en voor buisoven productieapparatuur). De projectresultaten ondersteunen in het algemeen de Nederlandse industrie in het handhaven en versterken van haar huidige en toekomstige concurrentiepositie als leveranciers van apparatuur en technologie voor de PV-industrie.

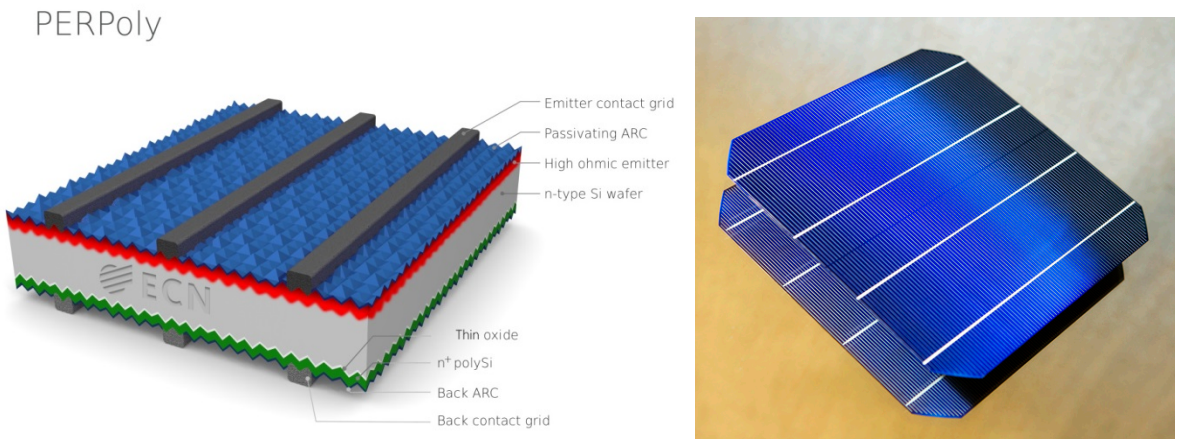

Fig. 1. Het celtype waarop dit project gericht was: een n-type bifacial zonnecel (door ECN als n-Pasha aangeduid; tegenwoordig is de meer generieke naam n-PERT gebruikelijker, acronym voor n-type zonnecel met Passivated Emitter and Rear Totally diffused) met achterzijde polysilicon passivated contact. Links: schematische dwarsdoorsnede . Rechts: foto.

Beschrijving van de behaalde resultaten, de knelpunten en het perspectief voor toepassing

Een inleiding tot het onderzoeksgebied en belangrijke projectresultaten worden uitgebreid in de volgende drie artikelen beschreven.

Inleiding tot gepassiveerde contacten, en polysilicium in het bijzonder.

(herdruk uit het Nederlands Tijdschrift voor Natuurkunde, Februari 2017)

Op zoek naar contacten voor zonnecellen

In de zonnecelindustrie neemt het conversierendement jaarlijks met zo'n 2-3% (0,5% procentpunt) toe. Producenten en de R&D-gemeenschap zijn zeer gemotiveerd om de technologie voortdurend te verbeteren en daarmee deze gestage groei van het rendement te continueren. In de inspanningen gericht op hogere zonnecelrendementen komen de elektrische contacten van de zonnecel prominent naar voren. Naarmate andere verliesmechanismen worden verminderd, komen de overblijvende verliesmechanismen relatief en zelfs absoluut sterker naar voren. Contacten – die aan verscheidene, lastig te verenigen eisen moeten voldoen – geven aanleiding tot een belangrijk maar lastig te vermijden verliesmechanisme. Ze spelen daarom meer en meer een hoofdrol in de zoektocht naar hogere rendementen.

Bart Geerligs, Maciej Stodolny, Yu Wu, Astrid Gutjahr, Ingrid Romijn, Gaby Janssen, Martijn Lenes en Jan-Marc Luchies.

Stroom door zonnecellen opgewekt uit zonlicht via het fotovoltaïsche effect – deze technologie wordt in dit artikel zoals gebruikelijk als pv- of 'zonnestroom'-technologie aangeduid – levert in veel scenario's een belangrijke bijdrage aan de toekomstige wereldenergievoorziening [1]. Vanwege de enorme hoeveelheid zonnestraling die op het aardoppervlak invalt (afhankelijk van de geografische locatie ongeveer 1000 - 2000 kWh/m^2 per jaar) neemt pv zelfs relatief weinig oppervlak in beslag voor elektriciteitsopwekking in vergelijking met bijvoorbeeld biomassa en windenergie. In de afgelopen twee decennia is de groei van zonnestroomtechnologie daarom enorm geweest: het jaarlijkse productievolume is sinds het jaar 2000 met ongeveer een factor driehonderd toegenomen.

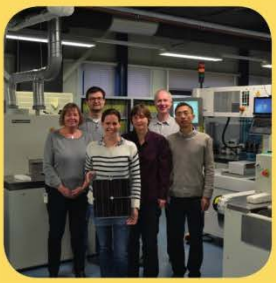

Bart Geerligs, Maciej Stodolny, Yu Wu, Astrid Gutjahr, Ingrid Romijn en Gaby Janssen doen onderzoek naar zonne-energie bij het Energieonderzoek Centrum Nederland (ECN) te Petten. ECN ontwikkelt kennis en technologie voor de transitie naar een duurzame energiehuishouding en slaat een brug tussen het fundamentele onderzoek in de universitaire wereld en de toepassing van nieuwe kennis en technologie in het bedrijfsleven. Martijn Lenes (Tempress Systems) en Jan-Marc Luchies (Amtech Systems) ontbreken op de foto.

geerligs@ecn.nl

Door verbeterde technologie, schaalvergroting en allerlei verbeteringen in de totale waardeketen zijn ook de kosten voor de opwekking van zonnestroom zeer sterk gedaald en kunnen pv-systemen in steeds meer markten concurreren. Wel zijn daarnaast netintegratie en energieopslag steeds belangrijker aspecten, die ook invloed op de kosten hebben.

Om de technologie en daarmee het rendement nog verder te verbeteren, wordt nu steeds vaker gekeken naar de contacten van zonnecellen. Figuur 1 laat het principe en belang hiervan zien. Een zonnecel functioneert op basis van een absorptiemateriaal, waarin fotonen worden omgezet in niet-evenwichtsladingdragers [3] (gaten en elektronen), en contacten die ofwel elektronen ofwel gaten transporteren naar het externe elektrische circuit waarop de zonnecel is aangesloten.

Verreweg het grootste deel van de wereldmarkt wordt ingenomen door zonnecellen op basis van wafers van

kristallijn silicium (c-Si), een materiaal waarin vanwege de indirecte bandkloof (*band gap*) niet-stralende recombinatie van gaten en elektronen via defecten erg relevant is. De dichtheid en 'recombinatie-activiteit' van defecten, zowel in de silicium wafer als aan het oppervlak, moeten dus geminimaliseerd worden. Dit is al goed mogelijk voor defecten binnen in de wafer en aan het oppervlak waar geen contacten in de buurt liggen. Voor defecten in de buurt van de contacten is de situatie lastiger omdat de contacten toestanden aan het waferoppervlak toegankelijk moeten maken voor ladingdragers in de wafer, om die ladingdragers te kunnen transporteren naar het externe elektrische circuit. Dat is lastig te verenigen met het vermijden van recombinatie via diezelfde toestanden. In de praktijk zijn de contacten daarom de belangrijkste bron van recombinatie voor zowel de monokristallijne industriële zonnecellen die vandaag de dag worden geproduceerd, als voor de beste laboratoriumzonnecellen.

Figuur 1 laat zien dat het doel van contacten is om één type ladingdrager met lage weerstand te geleiden naar één aansluiting van het externe circuit [4]. Het is essentieel dat het andere type ladingdrager niet in het hetzelfde contact terechtkomt; dat staat gelijk aan recombinatie. Deze eis houdt in dat de geleiding van ladingdragers naar een contact zo asymmetrisch mogelijk moet zijn. Er is een nauw verband tussen dit concept van asymmetrische geleiding en de passivering van het contact (vermijding van recombinatie bij het contact): als een ladingdrager in de buurt van het verkeerde contact recombineert, bijvoorbeeld op het grensvlak van de wafer en het contact, heeft dat ongeveer hetzelfde netto-effect als transport naar dat verkeerde contact. Vandaar dat de terminologieën ladingdragerselectieve contacten en gepassiveerde (of passiverende) contacten door elkaar gebruikt worden. Elk contact aan een zonnecel moet op z'n minst enige mate van ladingdragerselectiviteit en passivatie vertonen, anders is er geen sprake van een zonnecel. Hoe eenvoudig dit beeld ook mag lijken, het is nog steeds onderwerp van discussie. Contacten die extreem selectief zijn genereren momenteel veel interesse en enthousiasme in de R&D-gemeenschap en er wordt ook industrieel veel van verwacht.

Figuur 1 Schema van een zonnecel. Het laat zien hoe de werking van een zonnecel principieel berust op ladingdragerselectieve contacten. Recombinatie via defecten moet geminimaliseerd worden, wat in het geval van een kristallijn silicium zonnecel betekent dat het waferoppervlak gepassiveerd moet worden. Overgenomen met toestemming uit referentie [2].

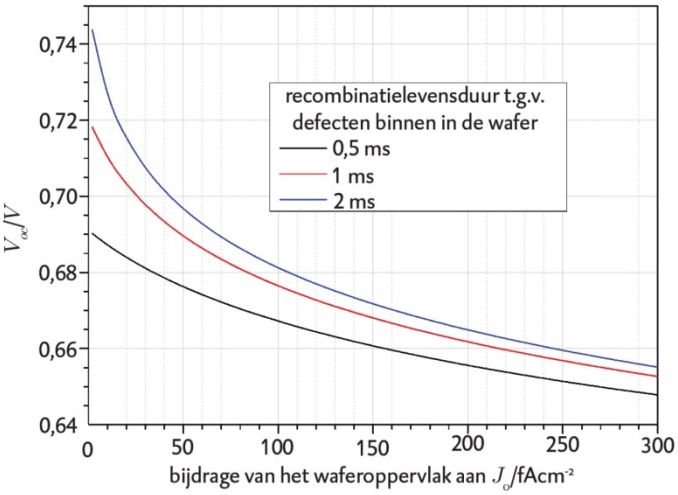

Figuur 2 Afhankelijkheid van de openklemspanning van een kristallijn silicium zonnecel van recombinatie, uitgesplitst naar oppervlakte- en bulkrecombinatie. De drie curves corresponderen met representatieve bulkrecombinatielevensduren in monokristallijne wafers.

De recombinatiestroom

De stroom-spanningkarakteristiek van een belichte zonnecel kan vereenvoudigd in het ééndiode-model worden beschreven door

$$J = J_{sc} - J_0\left[\exp\left(\frac{V}{kT/q}\right) - 1\right].$$

Hieruit kunnen we afleiden dat de openklemspanning gegeven wordt door

$$V_{oc} \approx \frac{kT}{q}\ln\left(\frac{J_{sc}}{J_0}\right),$$

waarin J_{sc} de kortsluitstroomdichtheid is, V de spanning, k de constante van Boltzmann, T de temperatuur en q de elektronlading. De parameter J_0 is de zogenoemde 'prefactor van de recombinatiestroom', die onder redelijke vereenvoudigingen als een optelling van oppervlakte- en bulkbijdragen berekend kan worden.

In de meeste zonnecellen is J_{sc} voornamelijk bepaald door reflectie- en absorptieverliezen en al vrij dicht in de buurt van de theoretische limiet [5]. De openklemspanning is sterk afhankelijk van de recombinatiestroom. Het rendement van een zonnecel is gedefinieerd onder een gestandaardiseerde belichting van 1000 W/m^2 als $J_{sc} \times V_{oc} \times$ FF/(1000 W/m^2). Hierin is de FF de 'vulfactor' die beschrijft hoe 'vierkant' de vorm van de stroomspanningskarakteristiek is. De FF is meestal iets groter dan 80%, afhankelijk van de serieweerstand. Figuur 2 laat de

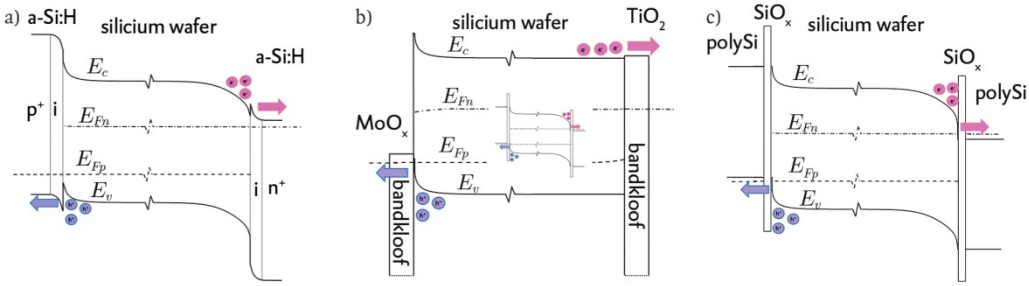

Figuur 3 **Varianten van gepassiveerde contacten die de werking via werkfunctie van het contactmateriaal en onderdrukking van geleiding door een barrière illustreren [7]. a) a-Si/c-Si heterojunctie, b) MoO_x gatencontact en TiO_x elektronencontact en c) hooggedoteerd polysilicium. In het polysilicium contact en de a-Si/c-Si heterojunctie zijn de barrières (respectievelijk intrinsiek a-Si en SiO) expliciet weergegeven, in (b) niet, maar ook daar kunnen ze aangebracht worden ter verbetering van de selectiviteit. De quasi-Ferminiveaus E_{Fp} en E_{Fn} tonen de elektrochemische potentiaal van respectievelijk de gaten en elektronen in de wafer en sluiten aan (niet getekend) op de potentiaal van het metallische contactmateriaal (niet getekend) dat aangebracht wordt op het selectieve contactmateriaal voor de betreffende ladingdrager.**

relatie tussen V_{oc} en J_0 zien voor een zonnecel op basis van kristallijn silicium. De meeste industriële zonnecellen hebben momenteel een V_{oc} rond de 0,65 V.

De kwaliteit van de bulk van de huidige wafers voor zonnecellen kan al zo goed zijn dat recombinatie voornamelijk plaatsvindt aan de voor- en achterzijde van het waferoppervlak. Ook de prefactor van de recombinatiestroom van die oppervlakken kan weer uitgesplitst worden, namelijk in de bijdragen van de niet-gecontacteerde en gecontacteerde delen, waarvan de laatste domineren. Zoals te zien is in figuur 2 kan een extreme vermindering van J_0 een grote bijdrage leveren aan de toename van V_{oc} en daarmee aan de trend van de toename van het rendement.

Principes van gepassiveerde contacten

De onderdrukking van de geleiding van één type ladingdragers naar een contact kan gebaseerd worden op een verlaging van de concentratie en/of mobiliteit van dat type ladingdragers in het gebied aansluitend aan het contact. De concentratie van één type ladingdragers wordt bij traditionele contacten aan zonnecellen verminderd door dotering met de tegengestelde polariteit in het silicium aansluitend aan het contact (dus om bijvoorbeeld de concentratie van gaten te verminderen, wordt het silicium onder het contact n-type gedoteerd). Dit heeft verschillende nadelen, onder andere dat de vermindering van ladingdragerconcentratie nogal beperkt is en dat het zorgt voor toename van Augerrecombinatieprocessen [6]. Om te relateren aan figuur 2: zulke contacten geven een bijdrage aan de J_0 van de zonnecel van typisch ongeveer 100 fA/cm². In het huidige onderzoek naar gepassiveerde contacten wordt de concentratie vaak verminderd door contactmaterialen met geschikte werkfunctie te gebruiken: een kleine werkfunctie onderdrukt de concentratie van gaten, terwijl een grote werkfunctie de concentratie onderdrukt van elektronen in het silicium onder het contact. De mobiliteit wordt vaak beperkt door een barrièrelaag te introduceren tussen de wafer en het contactmateriaal. Als een barrièrelaag wordt gebruikt, vermindert dit echter niet noodzakelijk de concentratie van één type ladingdrager aan het grensvlak met de wafer, dus het is eigenlijk altijd essentieel dat dat grensvlak zo goed mogelijk vrij van defecten is die recombinatie kunnen geven. Als een barrièrelaag wordt gecombineerd met een contactmateriaal met geschikte werkfunctie dan wordt de gevoeligheid voor defecten aan het grensvlak verminderd, en die combinaties geven in de praktijk de beste gepassiveerde contacten.

Figuur 3 illustreert een aantal concepten voor gepassiveerde contacten die momenteel sterk in de belangstelling staan. De Nederlandse academische wereld doet samen met ECN en het Nederlandse bedrijfsleven volop onderzoek naar veel van deze concepten. Het doel is technologieën te vinden die een J_0 van liefst (veel) lager dan 10 fA/cm² kunnen geven. Er zijn natuurlijk bijkomende eisen, zoals dat de technologie robuust en goedkoop industrialiseerbaar moet zijn, het contactmateriaal geen optische absorptie geeft (vooral als het gebruikt gaat worden aan de voorzijde van een zonnecel), geen ongewenste interacties met de rest van de zonnecel heeft et cetera.

Polysilicium

Een buitengewoon effectief materiaal voor een passiverend contact is een film hoog gedoteerd silicium (n-type voor kleine werkfunctie dus elektronencontact, p-type voor grote werkfunctie dus gatencontact) van typisch 10 - 200 nm dikte die door een dun oxide van de wafer wordt gescheiden (figuur 3c en figuur 4). Dit sluit technologisch goed aan op de standaard c-Si-zonnecelproductietechnologie. De film hoog gedoteerd silicium kan door *low pressure chemical vapour deposition* (LPCVD) worden gedeponeerd, resulterend in polykristallijn silicium (polysilicium). De opstapeling wafer/oxide/polysilicium heeft enige verwantschap met een (*leaky*) *gate*-structuur van MOSFET's (*metal-oxide-semiconductor field-effect transistor*). De hoge dotering in het polysilicium geeft de vereiste vermindering van de concentratie van één type ladingdrager in de wafer aangrenzend aan het contact. De oxidebarrièrelaag zorgt voor een lage defectdichtheid en dus lage recombinatie op het grensvlak met de wafer. De belangrijke rol van het dunne oxide is daarnaast om transport van de ladingdragers te beperken. Het is wat dat betreft vermoedelijk weinig selectief, maar door het grote verschil in concentratie van beide types ladingdragers in het silicium aangrenzend aan het oxide (vanwege de dotering in het polysilicium) kan het oxide zo geprepareerd worden dat er

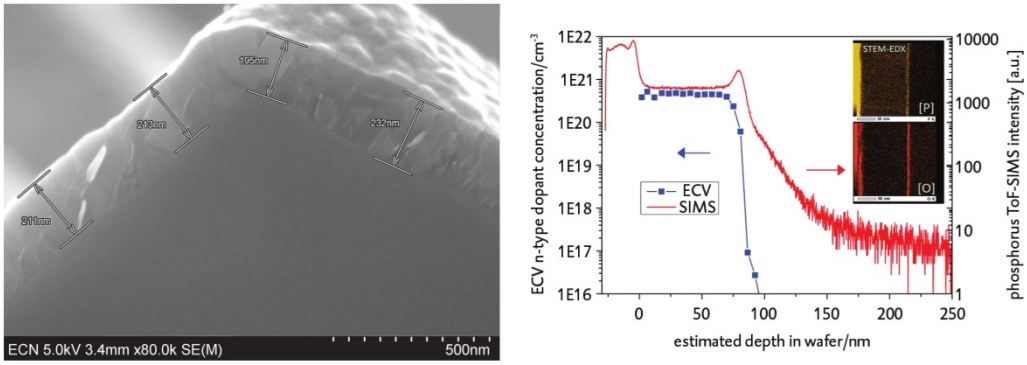

Figuur 4 **Links: elektronenmicroscopieopname van een dwarsdoorsnede van een polysilicium contact op een textuurfacet van een zonnecel. Op het grensvlak van het polysilicium en de wafer bevindt zich een circa 1,3 nm dik oxide. Rechts: SIMS- en ECV-metingen van het doteringsprofiel in een polysilicium contact tonen dat het goed mogelijk is om de dotering in het polysilicium 'op te sluiten', wat helpt om Augerrecombinatie in de wafer te minimaliseren. Secondaire ionenmassaspectroscopie (SIMS) toont de totale concentratie fosforatomen, elektrochemische capaciteitspanningprofilering (ECV) toont de concentratie n-type-dotering in het silicium. SIMS en STEM-EDX tonen ook (voor depth < 0) het fosforrijke siliciumoxide dat fungeerde als bron voor de fosfordiffusie in het polysilicum. De STEM-EDX-opname toont net als het SIMS-profiel dat dotering zich enigszins ophoopt aan het grensvlak, echter zonder te veel recombinatie-actieve defecten te creëren.**

voor meerderheidsladingdragers nog niet te veel serieweerstand optreedt, maar dat de niet-gewenste ladingdragers nauwelijks in het polysilicium terechtkomen. In dat geval veroorzaken Augerprocessen, defecten in het polysilicium en de metallische contacten op het polysilicium geen merkbare recombinatiestroom.

Hoewel deze polysiliciumtechnologie al lang bekend is om de donkerstroom van bipolaire transistoren te verlagen, is de potentie voor de pv-industrie lange tijd over het hoofd gezien door een groot deel van de R&D-gemeenschap. De polysiliciumtechnologie is (in tegenstelling tot bijvoorbeeld de a-Si/c-Si-heterojunctietechnologie) compatibel met het gebruik van relatief hoge procestemperaturen, die in de zonnecelproductie gebruikt worden voor dotering, aanbrengen van antireflectiecoating, aanbrengen van metaalcontacten, solderen en laminatie van zonnepanelen. Dit zorgt ervoor dat deze technologie snel geadopteerd kan worden en daarmee extra veelbelovend is.

De polysiliciumtechnologie is onder andere beschikbaar door middel van LPCVD-reactoren en diffusieovens van Tempress Systems BV, een belangrijke Nederlandse partij op de wereldmarkt van apparatuur voor zonnecelproductie. Tempress, ECN en de drie Nederlandse technische universiteiten zijn momenteel intensief bezig met het onderzoeken, toepassen en verfijnen van de polysiliciumtechnologie voor zonnecellen. Een van de eerste toepassingen was het vervangen van de traditionele achterzijde van een hoogrendementszonnecel, resulterend in een zogenoemde PERPoly-zonnecel (figuur 5) [8].

De totale J_o van de zonnecel werd hierdoor gehalveerd van ongeveer 200 naar 100 fA/cm^2, resulterend in een verbetering van circa 15 mV van de uitgangsspanning. Wel nam de externe quantumefficiëntie wat af in het infrarood vanwege fotonabsorptie door vrije ladingsdragers (*free carrier absorption*). Het rendement steeg met circa 0,4 procentpunt tot 21,3%. We zien hier twee belangrijke aspecten en onderzoeksonderwerpen voor de huidige praktische ontwikkeling van gepassiveerde contacten: 1) de voorzijde J_o was ongewijzigd circa 100 fA/cm^2, wat het profijt van de verbetering van de achterzijde beperkte; 2) de zware dotering in het polysilicium resulteert in merkbare infraroodabsorptie door vrije ladingdragers. Een derde belangrijk aspect, dat in dit resultaat nog niet zo in het oog springt, is dat de metaalcontacten op het polysilicium momenteel toch nog enige bijdrage aan J_o geven; dit is typisch voor hedendaagse contacttechnologie die gebaseerd is op metaalpasta's die zich enigszins inetsen in het silicium.

De J_o-bijdrage van de polysilicium film op de achterzijde van de cel in figuur 5 is ongeveer 7 fA/cm^2. ECN heeft op vlakke (ongetextureerde) silicium wafers een J_o bereikt van minder dan 1 fA/cm^2. Dit komt dicht in de buurt van de radiatieve limiet (de limiterende stralende recombinatie) van silicium van 0,27 fA/cm^2. Vanuit dat oogpunt is polysilicium dus een buitengewoon ideaal contact.

Het belangrijkste principiële pijnpunt van polysilicium is dat het in de praktijk eigenlijk niet op de voorzijde van een zonnecel gebruikt kan worden, omdat elke fotonconversie die plaatsvindt in het polysilicium in plaats van in de wafer, resulteert in verlies (de in het polysilicium gegenereerde ladingdragers recombineren voordat ze de wafer bereiken). Polysilicium absorbeert een significante fractie van het uv- en zichtbaar licht. Er zijn twee oplossingsrichtingen: 1) breng beide contacten naar de achterzijde (een *all-back-contact* zonnecel, die er ook nog eens aantrekkelijker uitziet); 2) ontwikkel een passiverend contact van hoge kwaliteit voor de voorzijde, dat veel transparanter is voor korte golflengtes dan polysilicium. Aan beide oplossingen werkt ECN zeer actief, met industriële en academische partners. De TU Delft heeft al laboratoriumresultaten gepubliceerd van dergelijke polysilicium zonnecellen waarbij beide contacten aan de achterkant zijn geplaatst [9]. De TU Eindhoven is gespecialiseerd in atoomlaagdeposities van zeer dunne lagen, waaronder de eerder genoemde metaaloxides TiO_x en MoO_x (zie figuur 3b) [7,10,11], die gebruikt kunnen worden voor een gepassiveerd contact dat veel transparanter is dan polysilicium.

Een aardige uitwijkmogelijkheid om het volle profijt van polysiliciumpassi-

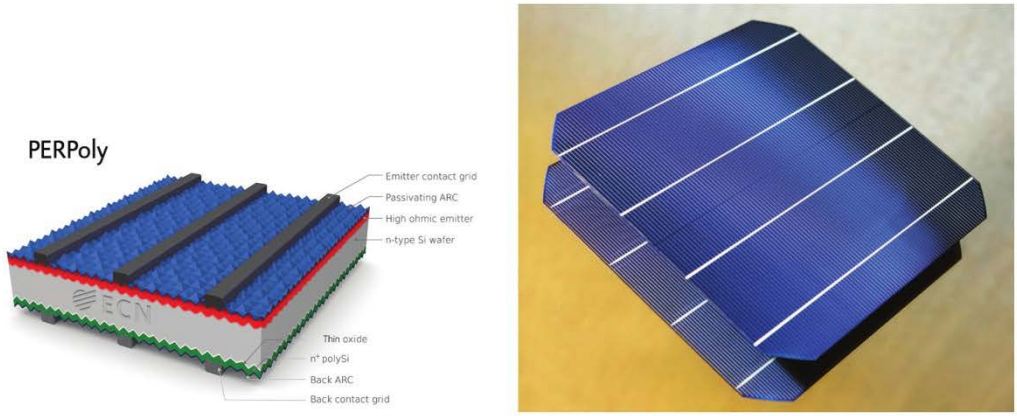

Figuur 5 PERPoly-zonnecel geproduceerd in samenwerking tussen ECN en Tempress Systems. Links: schematische weergave. Op de achterzijde bevindt zich een door n-type polysilicium gepassiveerd contact in plaats van een conventioneel gediffundeerd contact. Voor- en achterzijde zijn getextureerd met pyramidevormige oppervlaktestructuren voor betere lichtinvanging. ARC staat voor antireflectiecoating. Rechts: foto boven reflecterende achtergrond. De afmeting is de gebruikelijke afmeting voor industriële zonnecellen: 156 mm x 156 mm.

vering ook aan de voorzijde van de cel te kunnen gebruiken, zonder de nadelen, is toepassing in een tandem-zonnecel. Hierin wordt een semitransparante zonnecel met grotere bandkloof dan silicium boven de silicium zonnecel geplaatst. De fotonen die anders in het polysilicium zouden worden geabsorbeerd, worden dan in de bovenste zonnecel geabsorbeerd en nuttig omgezet in elektrische stroom. Ook tandems zijn een actief onderzoeksonderwerp, waarmee het de bedoeling is rendementen van 30% of misschien zelfs hoger te bereiken.

Wat betekent deze technologie voor de toekomst? De industrie is positief over introductie van polysiliciumgepassiveerde contacten op korte termijn. In samenwerking met een klant zijn van cellen met polysilicium contacten zonnepanelen gemaakt, die belangrijke duurzaamheidstesten doorstaan. We nemen de eerste signalen waar dat producten met polysilicium contacten eraan komen. Op middellange tot lange termijn lijkt het uitgesloten dat silicium zonnecellen níet op een bepaalde variëteit van zeer effectieve gepassiveerde contacten gebaseerd zullen zijn. Voor de komende jaren kan onderzoek naar gepassiveerde contacten daarmee een van de meest dankbare onderwerpen zijn voor materiaal-, natuur- en scheikundig onderzoek gericht op zonneceltoepassingen. Een stip op de horizon kan zijn dat productie van een silicium zonnecel met slechts een korte serie van eenvoudige en zeer goedkope applicatiestappen van gepassiveerde contactmaterialen op een silicium wafer plaatsvindt, bijvoorbeeld door zeefdrukken van twee organische halfgeleiders. Dit zou een revolutie in de silicium zonnecelwereld betekenen.

Referenties en noten

1 www.worldenergyoutlook.org.
2 Presentatie van van A. Cuevas *et al.* op de IEEE PV specialists conference, 2015.
3 In sommige types zonnecellen worden fotonen omgezet in excitonen.
4 U. Würfel, A. Cuevas en P. Würfel, *IEEE J. Photovoltaics* **5** (2015) 461.
5 De fotonflux van de zon op het aardoppervlak, voor fotonen met energie groter dan de bandgap van silicium, resulteert in maximaal circa 44 mA/cm^2.
6 Recombinatie van twee ladingdragers waarbij energie wordt overgedragen naar een derde ladingdrager. Vanwege de indirecte bandkloof van silicium is dit meestal het belangrijkste intrinsieke recombinatiemechanisme, belangrijker dan stralende recombinatie.
7 Zie bijvoorbeeld een korte review van J. Melskens *et al.*, DOI: 10.1109/PVSC.2015.7355646.
8 PERPoly is een door ECN geïntroduceerde afgeleide van de standaardbenamingen voor zonnecellen die ooit geïntroduceerd zijn door de University of New-South Wales en die wereldwijd gebruikt worden. PERPoly betekent *passivated emitter and rear polysilicon contact solar cell*. Voor resultaten zie bijvoorbeeld M. Stodolny *et al.*, *Solar Energy Materials and Solar Cells* **158** (2016) 24.
9 G. Yang *et al.*, *Solar Energy Materials and Solar Cells* **158** (2016) 84.
10 B. Macco, *et al*, *Phys. Stat. Sol. RRL* **9** (2015) 393.
11 Presentatie van J. Melskens *et al.* op de EU PVSEC, Hamburg, 2015.

Toepassing van de polySi laag in de n-Pasha zonnecel.

Resultaten gepubliceerd als “n-Type polysilicon passivating contact for industrial bifacial n-type solar cells”, door M.K. Stodolny et al., Solar Energy Materials and Solar Cells 158 (2016) 24-28.

Abstract

We present a high-performance bifacial n-type solar cell with n^+ polysilicon (polySi) back side passivating contacts and fire-through screen-printed metallization, processed on 6" Cz wafers. The cells were manufactured with low-cost industrial process steps yielding a best efficiency of 20.7%, and an average V_{oc} of 674 mV. A specific edge isolation process step was not required. We analysed effects of variation of doping level, thickness, and oxide properties of the n-type polySi/SiO_x layers, as well as hydrogenation from a PECVD SiN_x:H coating, which led to recombination current densities down to ~2 fA/cm^2 and ~4 fA/cm^2 on planar and textured surface, respectively. The results are novel in four aspects: the cells are bifacial, they are full 6" size while employing LPCVD for the polySi deposition, the polySi passivating contact is metallized by fire-through screen printing paste, and hydrogenation is done by PECVD-deposited and fired SiN_x:H. Analysis shows that the wafer bulk lifetime in the cell is high and that the V_{oc} of the cell is limited by the J_o of the uniform diffused boron emitter and its contacts. Ways to improve the efficiency of the cell to > 22% are indicated.

1. Introduction

The combination of a thin oxide (SiO_x) and doped polysilicon (polySi) to obtain low recombination junctions, originating from early work on bipolar transistors [1], was demonstrated in the 1990s to be a viable candidate for creating passivating contacts to crystalline silicon (cSi) solar cells [2,3].

A key element in the passivating contact structure is the thin oxide layer which has a reasonably low density of interface defects (D_{it}), supported by a hydrogenation step (typical models estimate a surface recombination velocity (S) of ~10^3-10^4 cm/s). This thin oxide layer serves also as a tuneable diffusion barrier, which is indispensable for keeping most of the dopant within the polySi layer thus avoiding creation of a typical diffused junction in the wafer. The doped polySi layer, due to the induced field effect, reduces minority carrier density at the interface with the wafer while providing good conductance for the majority carriers to the contacts applied on the polySi.

The combination of the interfacial thin oxide with doped polySi provides a low transmission of minority carriers assuring therefore a minimal recombination in polySi and at the metal contact. Together with the low level penetration of dopants in the wafer, this results in excellent passivation. The oxide/polySi stacks can be contacted by metal without increasing the recombination of minority carriers generated in the cSi wafer.

Recent progress on cells with such contacts, achieving conversion efficiencies above 25% on small area cells [4,5], and demonstrating in excess of 21% cell efficiency on 6" monofacial cells [6], merit the need to investigate industrialization of the concept.

The purpose of the work in the present paper is to understand practical optimization routes, using solely high volume production proven equipment, for the n-type polySi passivating contact as well as to demonstrate potential industrial cells with such a back contact. In this work we employ a polySi layer grown in a low pressure chemical vapor deposition (LPCVD) furnace which is subsequently doped by means of $POCl_3$ diffusion.

Specifically, optimization of the thin oxide properties, polySi thickness and phosphorous (Ph) doping level, hydrogenation from SiN_x:H, and contacting of the polySi are investigated. The evaluation of the feasibility of firing-through screen-printed metallization on polySi (without adding significant contact recombination) is included. The n-type polySi with screen printed contacts is integrated on the back of a cell with a boron emitter made by an industrial diffusion process, thus leading to a novel low-cost but high performance solar cell concept.

High efficiency solar cells made with LPCVD based polySi layers and screen printed fire-through contacts have several advantages, amongst others they can be realized by modest adaptation of conventional screen-print solar cell processes. LPCVD is a well-established high-throughput industrial process that can be easily implemented in state of the art solar cell manufacturing lines.

2. Material and methods

2.1 LPCVD polySi layers

PolySi layers were produced in a high-throughput industrial LPCVD furnace and subsequently doped by means of $POCl_3$ diffusion [7]. An LPCVD process has the benefit of creating very conformal and pinhole-free layers. This ensures that the underlying interfacial oxide is protected against subsequent doping steps and chemical treatments. For mass production, batches of up to a few hundred wafers can be processed simultaneously with excellent process uniformity. The thin oxide was produced by thermal oxidation (Th.Ox) or wet chemical oxidation (NAOS). A reliable absolute thickness measurement is not well feasible, but the thickness was estimated from spectroscopic ellipsometry on mirror polished wafers to be 13 to 15 Å. The high repeatability and tuning of this thickness at the single Å level is possible as well as necessary and will be addressed in the near future..

The effect of variations of process parameters on the recombination parameter J_o was characterized at lifetime level by photoconductance measurements (Sinton WCT-120 tool) and photoluminescence (PL), and related to the dopant profile measured by ECV (electrochemical capacitance-voltage). The best process parameters in terms of resulting J_o were applied at cell level.

2.2. Investigation of polySi doping and passivation

Symmetrical lifetime samples were fabricated on 5 Ω·cm n-type 6" Czochralski (Cz) wafers. The thickness of chemically polished wafers was 150 µm and of textured wafers 175 µm. After the wet-chemical oxide or thermal oxide was grown, a 70 or 200 nm thick intrinsic polySi layer was deposited by LPCVD, followed by $POCl_3$ diffusions at 3 different temperatures resulting in polySi layers with different dopant concentrations and sheet resistances (R_{sheet}, measured using a Sherescan tool), as well as different phosphorous leakage through the thin oxide into the wafer (measured using ECV).

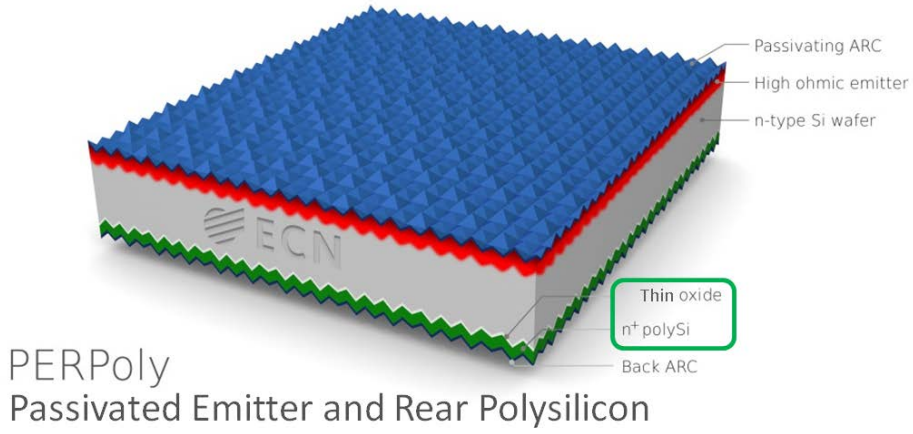

FIG. 1. Schematic drawing of the bifacial n-type solar cell design of this paper, featuring n-polySi\SiO_x contacts, named PERPoly (Passivated Emitter and Rear Polysilicon).

2.3. Application in industrial bifacial n-type cells

239 cm^2 n-type solar cells were produced according to standard industrial process steps with the exception of replacing a diffused Back Surface Field (BSF) with n-type doped polySi/SiO_x contacts, as shown in Fig.1. Such device can be called PERPoly (Passivated Emitter and Rear Polysilicon). In the cell process tests we have so far only employed the 200 nm polySi thickness. The cell processes stay close to existing industrial n-type technology, by employing only PV

process tools that are proven for low-cost high-throughput production. A specific edge isolation process step was not required. The metal grid was screen-printed using fire-through pastes both to contact the B-emitter on front and polySi on back. The co-firing process was optimized and the settings are similar to the industrial standards.

3. Results and discussion

3.1. PolySi doping and passivation

Fig. 2. shows the resulting active phosphorus concentration profiles, measured with ECV on the chemically polished samples, for three different diffusion runs. Increasing diffusion temperature resulted in higher active phosphorus concentration within the polySi layer with an abrupt drop indicating the location of the Th.Ox, but with noticeable phosphorous-indiffusion especially in case of NAOS (we call this a 'leaky profile'). Fig. 2 also shows the corresponding R_{sheet} values. For the thickest (200 nm) polySi increasing the temperature of the diffusion resulted in an increased dopant concentration. However, for the thinner (70 nm) polySi similar concentrations were found for all diffusion processes applied. This leads us to believe the doping level in the thick polySi layers is limited due to the amount of phosphorus available. Despite similar dopant concentrations, the thin polySi layers still show a decrease in sheet resistance (from 302 to 156 Ω/sq). This indicates that higher diffusion temperatures are resulting in higher charge carrier mobilities likely due to continued crystallization of the polySi.

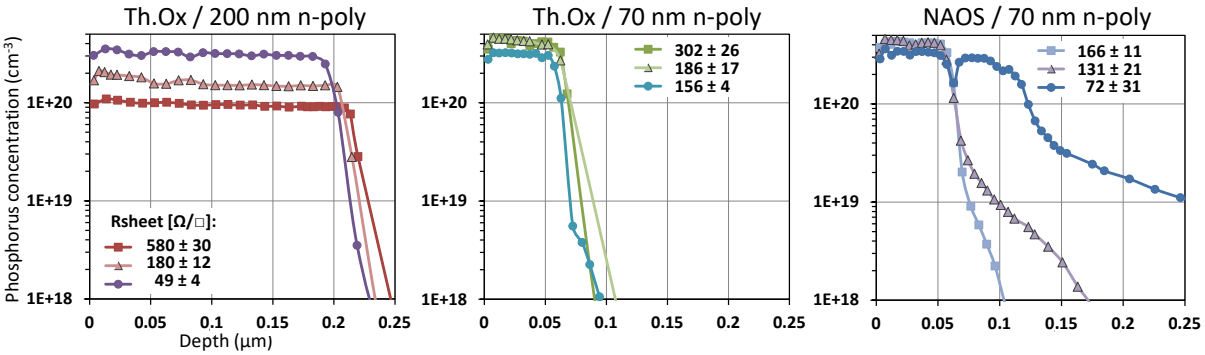

FIG. 2. Phosphorus doping profiles investigated for the polySi/SiO_x/Cz-Si carrier selective structures with the corresponding R_{sheet} values, on polished wafers.

Fig. 3 presents the evolution of the recombination parameter J_o (the dark saturation current) for the investigated n-polySi/SiO_x structures through various subsequent processing steps, again for chemically *polished* wafers. All J_o, iV_{oc} and lifetime measurements presented here were obtained with the Sinton WCT-120 tester on symmetric lifetime samples.

Average J_o per side <10 fA/cm^2 was achieved already without any particular hydrogenation steps, i.e. right after doping. We attribute the higher initial J_o of the 200 nm thick high R_{sheet} layers at least partly to the lower doping level which increases sensitivity to the interfacial D_{it}. For the 70 nm layers with Th.Ox there is little variation of doping level, and therefore little variation of initial J_o. The doping level for all those layers is in the same range as the heaviest doped 200 nm layer. As expected from the Debye length of only a few nm in the polySi, no difference in J_o is observed for 70 and 200 nm polySi layer thickness. For the 70 nm thick layers on top of the NAOS oxide, the initial J_o (before hydrogenation) is probably dominated by effects of the phosphorus leakage through the thin oxide. A significant 'leaky diffusion profile' in the case of structures with the NAOS interfacial oxide and $POCl_3$ diffusion at highest temperature (72 Ω/sq) resulted in high J_o. This might be due to a significant Auger recombination in the wafer near to the surface and/or increased leakage of minority carriers through a damaged oxide increasing the amount of interface defect states. Interestingly, the moderate 'leaky diffusion profiles' of NAOS/polySi with R_{sheet} of 131 and 166 Ω/sq showed still relatively low J_o values.

Improvements in J_o were observed after SiN_x:H deposition. PECVD (plasma enhanced chemical vapour deposition) SiN_x:H resulted in improved J_o in particular for the 200 nm n-poly layers with low doping level and R_{sheet} of 580 and 180

Ω/sq. We attribute this to hydrogenation of the SiO_x/wafer interface. However, the hydrogenation from SiN_x:H did not completely mask effects from variations in D_{it} or doping level. Firing of the SiN_x:H layer did not significantly change J_o. Removal of the SiN_x layer by wet chemical etching did not change J_o, as might be expected since this should not change the hydrogen passivation of defects at the SiO_x/wafer interface, protected by the polySi top layer. This indicates that the passivation of the outer surface of the polySi is irrelevant, validating the concept of the passivating contact.

In conclusion, it should be noted that low sheet resistances could be combined with excellent J_o for some of the investigated thin polySi layers. This allows us to use a partially contacted back (open grid on the back of the cell, resulting in a bifacial cell) which is a practically useful novelty in the field of polySi.

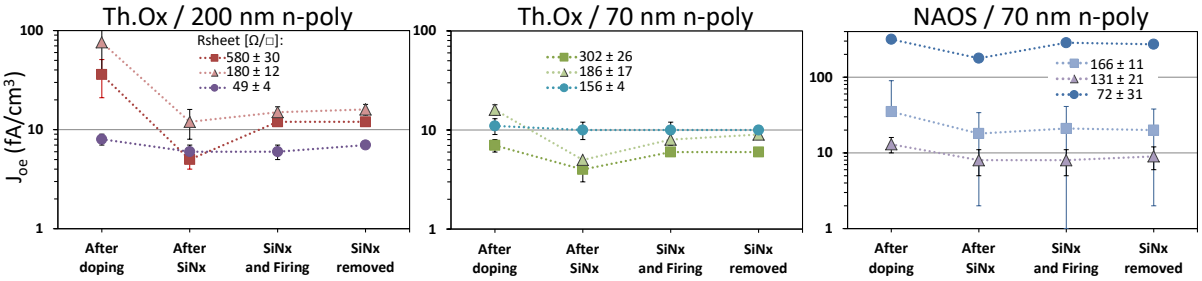

FIG. 3. Evolution of surface passivation quality of studied polySi/SiO_x carrier selective structures on *polished* Cz-wafers in a sequence of process steps. All J_o values per side are average of up to 15 points on 3 wafers and error bars depict standard deviations.

TABLE I. Best passivation characteristics obtained on *polished* wafers. Symmetric wafer structures with n-polySi/SiO_x on both sides. "Lifetime"= effective minority carrier recombination lifetime.

Cell type (polished, Th.Ox)	iV_{oc} (mV)	$J_{oe\ n\text{-}poly}$ (fA/cm²)	*Lifetime* (ms @$\Delta n=10^{15}$ cm^{-3})
After doping (200 nm n-poly; 49 Ω/sq)	~731	~3.4	~5.0
After SiNx (70 nm n-poly; 186 Ω/sq)	**~743**	**~2.2**	~6.6
After SiNx and Firing (200 nm n-poly; 49 Ω/sq)	~734	~5.2	~9.4
After SiNx removed (200 nm n-poly; 49 Ω/sq)	~732	~3.0	**~12.3**

Table I shows a summary of the best passivation characteristics measured after these industrially relevant process steps on chemically *polished* wafers. After the phosphorus doping to 3×10^{20} cm^{-3} already a very low J_o of ~3 fA/cm² was achieved without any particular hydrogenation steps. Deposition of SiN_x:H reduced the best value of J_o further to ~2 fA/cm². Firing seemed to improve the effective lifetime but somewhat increased the best value of J_o to ~5 fA/cm².

Fig. 4 shows the evolution of average J_o per side on *textured* wafers through industrial process steps relevant for a solar cell production. The n-polySi/SiO_x capped with SiN_x:H was highly robust and showed on average J_o~10-20 fA/cm² per side after firing, thus proving that a direct implementation of n-poly into an industrial solar cell production is feasible. Some degradation of J_o after fire-through of the contact grid on the n-polySi is visible, which will be discussed in section 3.3.

Table II shows the best passivation characteristics measured on *textured* wafers. Similar results were obtained for Th.Ox and NAOS, with 200 nm thick polySi layers after firing of SiN_x. The achieved recombination currents of ~4 fA/cm² are to our knowledge the best n-polySi passivation results on textured Cz-wafers so far reported.

TABLE II. Best passivation characteristics obtained on *textured* wafers. Symmetric wafer structures with n-polySi/SiO_x on both sides. "Lifetime"= effective minority carrier recombination lifetime.

Cell type (textured)	iV_{oc} (mV)	$J_{oe\ n\text{-}poly}$ (fA/cm^2)	*Lifetime* (ms @$\Delta n=10^{15}$ cm^{-3})
After SiNx fired (Th.Ox/200 nm n-poly; 39 Ω/sq)	~732	~4.2	~6.2
After SiNx fired (NAOS/200 nm n-poly; 71 Ω/sq)	~731	~4.3	~5.6

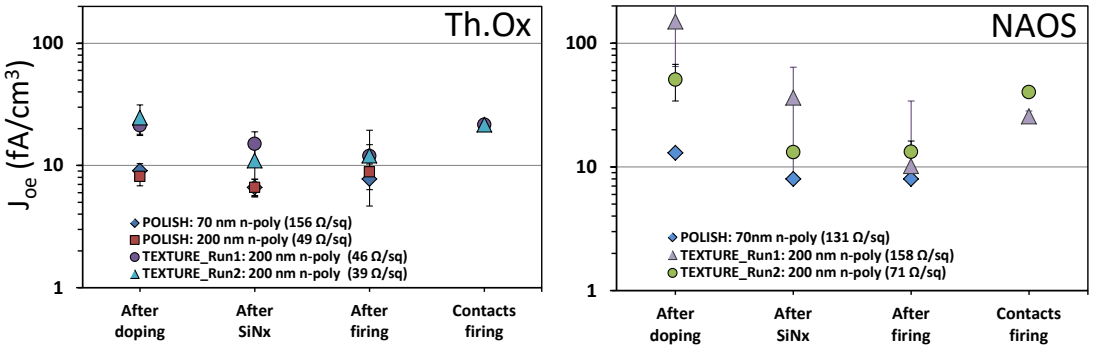

FIG. 4. Evolution of average J_o per side of studied polySi/SiO_x carrier selective structures on *textured* as well as chemically polished wafers for cell production relevant steps. All J_o values are average of up to 15 points on 3 wafers and error bars depict standard deviations.

3.2. Application of polySi in industrial bifacial n-type cells

n-type cells were produced on 6" Cz wafers of 5 Ohm·cm. An industrial type uniform diffused emitter with a sheet resistance of 70 Ohm/sq was employed on the front side. The emitter was passivated with Al_2O_3 deposited by ALD (Atomic Layer Deposition (Levitrack tool from Levitech)), coated with PECVD SiN_x:H. The back side polySi was also coated with SiN_x:H. Table III presents an overview of the best *I-V* results of screen-printed H-pattern contacts on both sides of bifacial cells obtained in two consecutive experimental runs.

The cells showed ~82% bifacial performance (with back full area 200 nm thick n-poly; 46 Ω/sq). This bifacial ratio is about 10% less than for equivalent n-PERT cells with diffused BSF, and this loss is in agreement with the estimated absorption of short wavelength photons in the polySi.

Analysis of the half-fabricates and cells shown in Table III indicated that performance limitations due to the diffused B-emitter and contact at the front side were dominant in both runs. In Run1 the sub-optimal bulk lifetime (~750 µs on average, possibly due to lack of phosphorus gettering) also played a role, resulting in an average iV_{oc} for half fabricated cells without contacts $iV_{oc}^{(\text{half-fab. without contacts})}$ of ~680 mV. In contrast, in Run2 the bulk lifetime was greatly improved (~3 ms on average) resulting in an average $iV_{oc}^{(\text{half-fab. without contacts})}$ of ~693 mV. Optimization of the cell process was carried out in Run2 to further exploit the excellent potential of the n-doped polySi/SiO_x back contact, yielding the best cell efficiency of 20.72% (spectral mismatch corrected, FhG ISE calibrated n-PERT reference cell, AAA Wacom system, in house) with cell V_{oc} of 675 mV. The cell efficiency distribution over the 6 cells with NAOS/n-polySi (71 Ω/sq) was 20.68 with a standard deviation of 0.05. In Run2 the Th.Ox was apparently slightly thicker than in Run1 as the FF was ~1% abs. lower than in Run1. The FF with NAOS/n-poly back contact in Run 2 is similar to typical *FF* for equivalent n-PERT cells with diffused BSF, and it seems there is no significant series resistance loss (more than about 0.1 Ohm·cm^2) in the polySi/NAOS/wafer junction. However, a full series resistance breakdown analysis is not yet completed for these cells.

Comparing J_o or iV_{oc} of 'half-fab. without contacts' with J_o or iV_{oc} of 'cell with contacts' in Table III and with the J_o with contacts in Fig. 4, shows that the losses related to the diffused B-emitter front side and front contact were dominant. Note that the J_o and iV_{oc} values given in Table III are best values (i.e., for best location on the wafer), while the V_{oc} for the cells with contacts are an average over the wafer due to the contact grids.

Furthermore some J_{sc} loss is due to non-contributing interband and free carrier absorption (FCA) in the polySi. The FCA in the n-polySi was evaluated by ray tracing analysis to be approx. 0.9 mA/cm^2 for 200 nm thickness and 3×10^{20} cm^{-3} phosphorus doping level. We intend to reduce this FCA by decreasing the polySi thickness and doping level. Table III illustrates the opportunity, through the experimental variation of J_{sc} as a function of the polySi doping level.

TABLE III. Parameters of textured bifacial solar cells with 200 nm rear polySi. Best cell results are shown as well as best J_o, iV_{oc} and bulk lifetime obtained on half-fabricates (obtained from QSSPCD, light I-V and SunsVoc measurements).

	J_{oe} *n-poly w/o contacts** (fA/cm^2)	J_o *F+B half-fab. w/o contacts** (fA/cm^2)	J_o *F+B cell w/ contacts**# (fA/cm^2)	*Bulk lifetime* (ms)	iV_{oc} *half-fab. w/o contacts** (mV)	iV_{oc} *cell w/ contacts**# (mV)	V_{oc} (mV)	J_{sc} (mA/cm^2)	*FF* (%)	*pFF* (%)	η (%)
Run1_Th.Ox/n-poly (46 Ω/sq)	9.7	64.7	~88	1.27	689	~679	669	37.5	78.7	81.4	19.75
Run1_NAOS/n-poly (158 Ω/sq)	7.9	63.9	~96	1.51	691	~672	665	38.2	77.8	81.9	19.77
Run2_Th.Ox/n-poly (39 Ω/sq)	5.1	58.9	~94	4.86	697	~675	673	38.4	77.8	82.8	20.09
Run2_NAOS/n-poly (71 Ω/sq)	7.7	56.2	~98	6.68	699	~680	675	38.8	79.1	82.8	20.72

F=front, B=back, *best spot, #QSSPCD measurements only on fingers-metal grid (not including busbars)

3.3. Outlook

Based on the obtained experimental results a qualitative description of key features of the passivating contact structures can be given.

The thin interfacial oxide layer needs to be thin enough not to limit the transmission of the majority carriers (allowing high *FF*) but should be dense/close enough to serve as a diffusion barrier, such that most of the doping is realized in the polySi layer. Slight dopant in-diffusion into the c-Si wafer (such as in the moderately leaky profile from Fig. 2c) is not harmful for the passivation properties and can be additionally beneficial for the transport of the majority carriers (perhaps avoiding transport via a tunneling mechanism only, allowing transport partially via less restrictive pinholes/percolation pathways [2]).

The polySi layer needs to be sufficiently high doped to allow adequate lateral transport for the application of bifacial grid metallization and also to provide a passivation boost by reducing the minority carrier density through the "field effect passivation". The thickness of polySi needs to be sufficient to block the penetration of the fire-through paste to the thin oxide interface. In our case 200 nm was sufficient, but we expect that thinner polySi will also be suitable. We have not yet attempted to make cells with the 70 nm polySi layers reported in this work. Also, the polySi thickness needs to be sufficient to allow the growth of phosphosilicate glass as a phosphorus dopant source, which is later on removed. On the other hand the thinner and the less doped the polySi layer, the lower parasitic absorption losses.

For the textured samples the hydrogenation of the interface defects is more critical, i.e., necessary for reaching very low J_o, compared to polished surfaces.

Fig. 5 presents a roadmap towards achieving 22%, which we have estimated assuming solely using industrial process equipment and materials. Firstly, the parasitic absorption in polySi can be reduced by making the layer thinner and less doped. Secondly, total J_o can be further reduced to 50 fA/cm^2 by implementing a higher R_{sheet} emitter and less penetrating fire-through pastes. Last but not least, the *FF* may be further improved by optimizing the thin interfacial oxide, and optimizing the front contacting grid design.

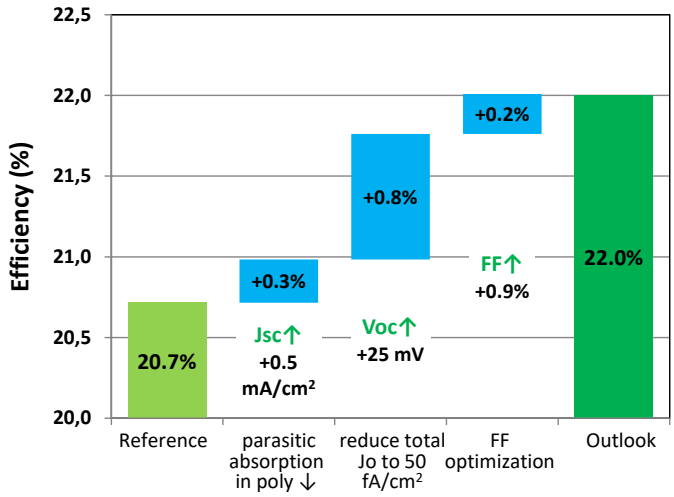

FIG. 5. Roadmap towards 22% PERPoly cell.

4. Conclusions

We presented studies of n-type polySi passivating contacts and their application on the back side of a high-performance bifacial n-type solar cell with fire-through screen-printed metallization, processed on 6" Cz wafers. The cell design is tentatively called PERPoly (Passivated Emitter Rear Polysilicon contact). The polySi/SiO_x passivating carrier selective contact structures were produced with a LPCVD-based process. The cell manufacturing further comprised, in addition to the LPCVD step, only processing on a small number of industrial tools, comparable to current n-PERT process flows on the market. A specific edge isolation process step was not required. A best efficiency of 20.7% was achieved together with very high average cell V_{oc} of 674 mV. As an added benefit, the cells are bifacial with bifaciality factor >0.8. To our best knowledge these are the first published results on 6" cells employing LPCVD for the polySi, and also the first published results of cells employing a polySi passivating contact with fire-through screen-printed metallization.

The polySi/SiOx passivating contact layers were investigated in detail by varying interfacial thin oxide growth method, polySi thickness and doping profile. Excellent passivation has been obtained both on polished and textured surfaces with recombination current densities J_o of ~2 fA/cm^2 and ~4 fA/cm^2, respectively. The effect of the fire-through grid on the J_o of the 200 nm thickness n-polySi contact was evaluated to be in the range of 10-30 fA/cm^2.

These results show the high potential of this technology to augment current cell processes, with large performance headroom for the future. Reaching 22% seems feasible by a number of improvements, especially on the emitter side. This brings the use of polySi passivating contacts closer to becoming a reality in low-cost industrial solar cell processing.

Acknowledgements

Part of this work was performed in the projects PV4facades (TEMW140009) and NexPas (TEZ0214002), which receive funding from the Topsector Energie of the Dutch Ministry of Economic Affairs. The authors acknowledge Teun Burgers for the ray tracing analysis of FCA in the polySi.

References

[1] P. Ashburn and B. Soerowirdjo, IEEE Transactions on Electron Devices, Vol. ED-31, no. 7, pp. 853-860, July 1984.
[2] E. Yablonovitch, R. M. Swanson and Y. H. Kwark, Proceedings of the 17th IEEE Photovoltaic/Spec. Conf., pp.1146 - 1148, 1984.
[3] J.Y. Gan and R.M. Swanson, 21st IEEE Photovoltaic Specialists Conference, Vol. 1, pp. 245-250, 1990.
[4] H. Steinkemper, F. Feldmann, M. Bivour and M. Hermle, IEEE Journal of Photovoltaics, Vol. 5, NO.5, pp.1348-1356, 2015.
[5] S. W. Glunz, F. Feldmann, A. Richter, M. Bivour, C. Reichel, H. Steinkemper, J. Benick, M. Hermle, 31st European Photovoltaic Solar Energy Conference and Exhibition, September 2015, Hamburg.
[6] Y. Tao, V. Upadhyaya, C.-W. Chen, A. Payne, E. L. Chang, A. Upadhyaya, A. Rohatgi, Prog. Photovolt: Res. Appl. (2016) published online, doi: 10.1002/pip.2739.
[7] M. Lenes, M. K. Stodolny, Y. Wu, L. J. Geerligs, J. R.M. Luchies, PV Asia, 29 Oct., 2015, Singapore

Studie van de eigenschappen van industriële metallisatie van polySi contacten.

Resultaten gepubliceerd als “Study of screen printed metallization for polysilcon based passivating contacts”, door H.E. Ciftpinar et al., Energy Procedia 124 (2017) 851-861.

Abstract

We investigate contacting of n- and p-type polysilicon (polySi) passivating contact layers with industrial screen-printed metal pastes, examining both fire through (FT) and non-fire through (NFT) pastes. The n- and p-type polySi layers, deposited by low pressure chemical vapour deposition and doped by $POCl_3$ diffusion, phosphorus implant, or BBr_3 diffusion, result in excellent J_o, even for 50 nm thickness (<2 fA/cm^2 for n-polySi, <10 fA/cm^2 for p-polySi). The contact recombination is investigated by photoluminescence, and by cell test structures to determine V_{oc} as a function of metallization fraction. The contact resistance is investigated by transfer length method (TLM). The contacts are also extensively studied by high resolution electron microscopy. All-polySi solar cells (i.e., cells with front and back carrier selective layers consisting of polySi) are prepared. Excellent implied V_{oc} values of nearly 730 mV and 710 mV are obtained on the un-metallized polished and textured cells, respectively. The contact recombination after applying screen printed metallization can be analyzed well with both methods (PL and V_{oc}-based) rendering values for the prefactor of the recombination current $J_{o,c}$ at the contact areas of about 400 and 350 fA/cm^2 for 200 nm thick n-polySi and p-polySi, respectively.

Introduction

Passivating contacts [1] can solve a main remaining hurdle that limits the efficiency of current industrial n-type silicon solar cells: carrier recombination at the electrical contacts [2]. Introduction of passivating contacts to industrial solar cell processing is thus very appealing, but it is demanding at the same time. It requires the passivating properties to be stable when metallized with industrial fire through (FT) paste in a high temperature firing step. One candidate for industrial passivating contacts is doped polysilicon (abbreviated as polySi in this article) on thin oxide [3], that has been shown to perform well at the rear side of PERPoly (Passivated Emitter Rear PolySilicon) solar cells metallized with industrial screen-print method [3], yielding in excess of 21% efficiency on 6 inch wafers [4].

In this paper, we study the contacting of polySi/SiO_x structures by screen printed metallization, and we present and compare suitable analysis methods of contact recombination. N- and p-polySi layers with different thicknesses were prepared on thin oxide on polished and textured wafers, showing excellent surface passivation. The contact resistance of metallization by fire through (FT) and non-fire through (NFT) screen-printed pastes on these polySi layers is tested by transfer length method (TLM), for both polySi dopant types, to confirm a proper contact formation. The contact recombination (expressed as the prefactor $J_{o,c}$ of the contact recombination current) is quantified by photoluminescence (PL) measurements supported by device modelling, as well as by V_{oc} measurements for various metal contact fractions on all-polySi solar cells (i.e., cells with front and back carrier selective layers consisting of polySi). Finally, a detailed SEM study is carried out to image the contact structure.

1. Experimental

2.1. PolySilicon processing and metallization schemes

The passivating contact test structures and cells were fabricated on 6’’ n-type solar grade Cz wafers, polished or textured, with a resistivity of 5 Ωcm. The thickness of chemically polished wafers was 160 µm and of textured wafers was 170 µm. Following the growth of a thin thermal oxide (Th.Ox), an intrinsic polySi layer was deposited with varying thicknesses (50, 75, 100, 125 and 200 nm) using low pressure chemical vapor deposition (LPCVD). For symmetrical samples the n-polySi layer was obtained by $POCl_3$ diffusion at 850°C, and p-polySi layers were obtained by BBr_3 diffusion at 880°C. For all-polySi cells (i.e., cells with front and back carrier selective Th.Ox/polySi stack) the n-type polySi was prepared by phosphorus implantation on one side (implant dose of 1E16 cm^{-2}, for 100 nm as well as

200 nm thickness) combined with an anneal provided by a BBr_3 diffusion at 880°C which also served as a doping source for creating p-polySi on the other side. The implant combined with BBr_3 diffusion resulted in n-poly and p-poly layers of similar doping levels as in the other experiments. The samples were characterized with electrochemical capacitance voltage (ECV) method for dopant profiles, and carrier lifetime measurements for implied V_{oc} (iV_{oc}) and passivation (J_o).

In order to investigate the impact of metallization on polySi properties, the polySi layers were contacted with industry-standard screen-printed fire through (FT) pastes, for contacting of phosphorus doped (Ag paste) or boron doped (AgAl paste) surfaces. Additionally, the samples with polished wafer surface were metallized with non-fire through (NFT) paste. Following glass removal and 80 nm SiN_x deposition using plasma enhanced chemical vapour deposition (PECVD) on both surfaces of the samples, FT-Ag and FT-Ag/Al paste was printed on one side of n-poly/wafer/n-poly, p-poly/wafer/p-poly and n-poly/wafer/p-poly samples with various test patterns to evaluate contacting and passivating properties. Samples metallized with NFT paste were subjected to a SiN_x patterning step prior to printing, to locally etch the SiN_x layer and provide direct access of the NFT Ag paste to the underlying polySi layer. Curing of NFT paste was done at different temperatures within a 610-650°C range. Firing of the FT pastes was done at various temperatures within 745-825°C range to investigate the temperature-dependence of contact resistance and recombination of the metallized surfaces.

2.2. Contact resistance and contact recombination measurements

Contact recombination was analysed with two approaches: i) by modelling of PL maps (GreatEyes-LumiSolarCell, coupled/calibrated with Sinton PCD measurements), and ii) by V_{oc} measurements for various metal coverage fractions. In case i) the (average) PL signal over metallization patterns with different metal coverage, applied on one side of samples with the same layers of polySi on both sides, was used for extraction of $J_{o,c}$. In case ii), FT grids were applied on both sides of all-polySi cells, to obtain $J_{o,c}$ using V_{oc} measurements. Fig. 1 illustrates the different metal patterns. Fig. 1(a) shows the patterns printed on one side of symmetrical samples for PL imaging and modelling. A 2 mm pitch pattern of Fig. 1(a) was subsequently cut into strips for TLM measurements. Fig. 1(b) shows the PL image of samples with a V_{oc} test pattern consisting of small cells with various finger fractions of 2, 4, 8, 16, 25 and 32% (for finger widths varying from 60 to 190 µm and pitches from 2 down to 0.4 mm) applied on one side of all-polySi cells. An H-pattern locally interrupted with metal free regions was printed on the other side. In addition to the test patterns, cells with on both sides a regular full-area H-pattern grid as shown in Fig. 1(c) were also prepared using the most promising temperature settings for firing/curing of the samples of Fig. 1(b). Contact resistivity (ρ_{co}) measurements were done using transfer length method (TLM, PVTools-TLM-SCAN).

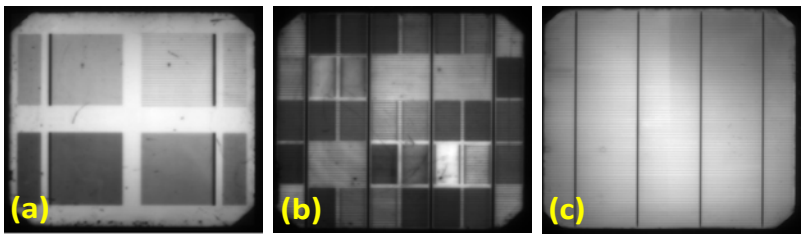

Fig. 1. PL images of textured wafers with 200 nm polySi passivating contacts, and printed FT metallization patterns. The metallization patterns consist of parallel fingers with varying pitches and widths. (a) 1-sided pattern used for PL analysis, 90 µm width fingers with pitches of 0.25, 0.5, 1 and 2 mm; (b) pattern with various metal fractions used for V_{oc} measurements; (c) pattern used for full-area cell metallization.

2.3. HR-SEM investigation of metallized polySi layers

Selected samples of all-polySi cells on polished and textured surfaces were sequentially repeatedly etched and imaged by high resolution scanning electroscope microscopy (HR-SEM), with top-view and cross-section images of the

contacted and non-contacted areas after each etching step. As the first step of sequential etching, exposed (bulk) metal was etched using aqua regia (HNO_3:HCl, 1:3); followed by imaging, and a second etching step of glass removal using hydrofluoric acid (5% HF) solution. After second imaging, in the third etching step, all remaining Ag and Ag/Al nanoparticle-agglomerates were etched by aqua regia, followed by final imaging.

3. Results and discussion

3.1. PolySi properties

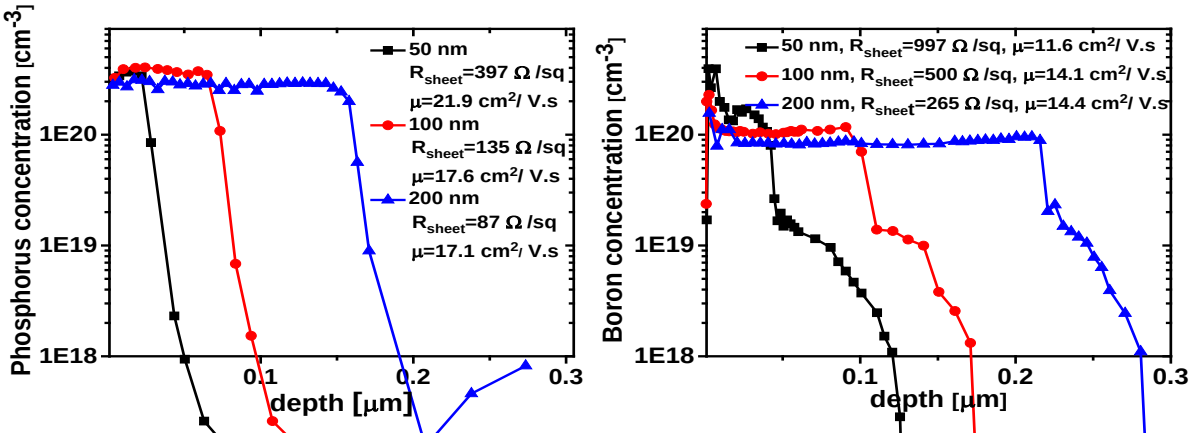

Fig.2. Doping profiles for the phosphorus (a) and boron (b) doped polySi/SiOx/Cz-Si carrier selective contact layers with their corresponding R_{sheet} values, on polished wafers. The nominal thickness of the polySi layers before the doping was 50 nm, 100 nm and 200 nm.

Fig.2 shows the active phosphorus and boron concentration profiles, measured with ECV, for polySi layers of three different thicknesses, deposited on chemically polished wafers. The n-polySi layers resulting after $POCl_3$ diffusion were thinner than the nominal deposited thickness due to a consumption of polySi by phosphosilicate glass (PSG) formation, whereas p-poly layers preserved roughly the nominal thickness, with a boron rich layer (BRL) observed at the top surface. We have verified, by comparison of STEM/EDX [5] and ECV, that an abrupt drop in doping concentration defines the location of polySi/SiO_x interface [4]. In the case of p-polySi the in-diffusion tails were substantial, which may be related to the higher temperature for B-diffusion compared to P-diffusion. Increasing the layer thickness t_{poly} from 50 to 200 nm reduced the sheet resistance (R_{sheet}) of the n-polySi layer from 397 to 87Ω/□, and from 997 to 265Ω/□ for the p-polySi layer. The mobility values in Fig. 2 were calculated from $\mu = 1/(R_{sheet}.t_{poly}.N_D.q)$, with N_D the average dopant concentration and q the elementary charge, and are about 3-4x reduced compared to c-Si, both for n-poly and p-poly. The passivation properties of the layers are shown in Table 1 in terms of prefactor of the dark recombination current (J_o) [6], and in terms of implied V_{oc} (iV_{oc}).

Providing SiN_x on both sides improved the iV_{oc} of all samples, with resulting highest values on polished samples of 744 mV for n-polySi and 725 mV for p-polySi, and corresponding J_o values of 0.6 fA/cm^2 and 7.3 fA/cm^2, respectively. Firing of the samples with PECVD SiN_x coating layers improved the performance of the p-polySi layers, with a reduction of J_o by 15-30%. Firing has a slightly detrimental effect on n-polySi passivation which we believe is due to some other factors related to $POCl_3$ diffusion that we are presently investigating, for example (re-) injection of gettered impurities. The inferior passivation properties of p-poly compared to n-poly are not fully understood.

Table 1. Best passivation characteristics obtained on chemically polished 5 Ω.cm n-type Cz wafers. Symmetric wafer structure with P- or B-doped polySi/SiOx on both sides. Overall best values are printed in bold.

	thickness	with glass		SiNx-as deposited		SiNx+firing	
	(nm)	iV_{oc} (mV)	J_o (fA/cm²)	iV_{oc} (mV)	J_o (fA/cm²)	iV_{oc} (mV)	J_o (fA/cm²)
n-poly	50	733	1.7	740	2.3	738	2.5
	100	731	**1.9**	744	**0.6**	742	**1.3**
	200	722	4.9	743	1.1	737	2.7
p-poly	50	707	**12.0**	724	7.8	728	6.2
	100	706	12.5	725	7.3	727	**5.1**
	200	705	12.8	726	**6.7**	728	5.7

3.2. *Contact resistance*

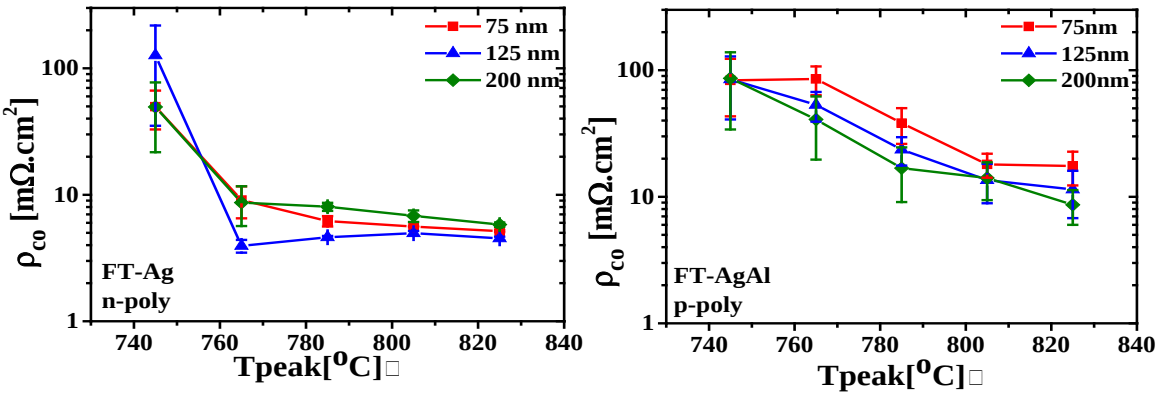

Fig. 3. Contact resistivity ρ_{co} of FT Ag paste on n-poly and AgAl paste on p-poly, on textured wafer surface, vs. firing temp (polySi is coated with SiN_x). Temperatures indicated are set points of peak temperature.

Fig. 3 shows contact resistivity ρ_{co} of Ag FT paste on n-poly and AgAl FT paste on p-poly, in dependence on the set peak firing temperature. Starting from 785°C, the contact resistance is significantly reduced for both polySi polarities and above 800°C it becomes roughly constant, at around 3-5 and 9-12 mΩ.cm² for n- and p-polySi respectively. These values are to be compared to typical ρ_{co} values of these pastes of 1-2 mΩ.cm² on n^+-diffused and 2-5 mΩ.cm² on p^+-diffused crystalline Si surfaces.

For the samples metallized with NFT paste on a polished wafer surface, TLM measurements of the contact on thin polySi layers (50 nm) resulted in ρ_{co} > 3000 mΩ.cm² for n-polySi and > 100 mΩ.cm² for p-polySi, whereas on thick (200 nm) layers values of ρ_{co} ~12 mΩ.cm² and ~26 mΩ.cm² were obtained for n-poly and p-poly, respectively. Improved contact resistivity on p-poly, down to ~9 mΩ.cm², was found on textured wafers. It should be noted that a dependence of ρ_{co} on the thickness or R_{sheet} of the polySi can be (partly) an artifact of the analysis method. The TLM analysis did not account for possible thinning of the polySi (resulting in an increase of the R_{sheet}) under the metallized finger, or for current pathways outside of the contacted polySi layer (which will depend on the polarity of the wafer). That means ρ_{co} could be overestimated [7].

3.3. Modelling of photoluminescence for extraction of $J_{o,c}$

The approach to PL modelling and extraction of $J_{o,c}$ from the PL measurements is to match Quokka [8, 9]-generated PL (*PLmod*) with experimental PL (*PLexp*), with $J_{o,c}$ as a variable. We use a Sinton PCD measurement to relate PL signal intensity to the surface passivation averaged over both sample surfaces ($J_{o,pas}$) prior to metallization. There are five different analysis locations on the samples as shown in Fig. 4.

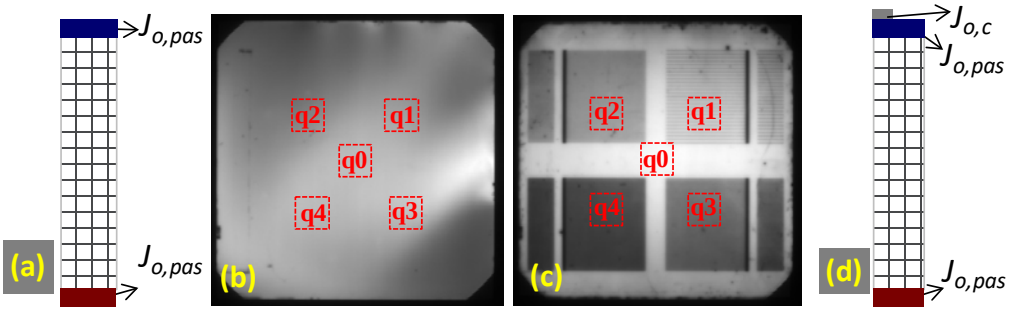

Fig. 4. Cross-sectional views of unit cells defined in Quokka before metallization (a) and after metallization+firing (d); PL images of symmetrical test structures before metallization (b) and after metallization+firing (c).

The sample before metallization is approximated by a symmetrical structure in Quokka as shown in Fig. 4(a), with the same R_{sheet} and $J_{o,pas}$ values for both surfaces, and with a fixed bulk lifetime of 3 ms. $J_{o,pas}$ is varied until modelled iV_{oc} is identical to measured one. Modelled $J_{o,pas}$ values were almost exactly the same as those obtained from Sinton PCD measurements. The PL emission in Quokka *(PLmod)* is used to calculate a calibration factor *N* that relates *PLmod* to the experimentally measured PL emission *PLexp* (locally, for each of the positions in Fig. 4(b)) as eq. (1).

$$N = \frac{PLmod}{PLexp} \tag{1}$$

N is subsequently used to relate *PLmod* to *PLexp* after metallization. Since the Sinton PCD measurement is no longer functional for the metallized regions [10], matching the Quokka-calculated PL emission with the experimental PL emission is used to find $J_{o,c}$.

Before extraction of $J_{o,c}$, an intermediate step is required to determine the effect of firing on passivation of non-metallized regions. Based on the results shown in Table 1, firing worsens passivation of non-metallized n-poly layers, while improving that of p-poly layers. For the PL samples after firing, the metal free region q0 in Fig. 4(c) is used to find $J_{o,pas}$ by matching *PLmod* and *PLexp*. The ratio of the two values of $J_{o,pas}$ obtained after and before firing is applied as correction factor to the $J_{o,pas}$ values in the modelling of the PL from the metallized regions q1-q4.

We have evaluated various approaches for extracting $J_{o,c}$ from modelling of PL measurements, with similar results. The approach presented here uses Quokka to model the area-averaged PL emission. In Quokka, an asymmetrical structure is defined using $J_{o,pas}$ (corrected for firing) for the whole rear side and the metal-free region on the front side, and $J_{o,c}$ for the metallized region on the front side. $J_{o,c}$ is determined so that the area-averaged PL emission in Quokka matches the measurement averaged over several fingers at some distance from the busbars. We have checked that variation of parameters for the PL emission model in Quokka have little effect on the outcome of this modelling. The result of the above described procedure is given in Fig. 5 for three different polySi thicknesses on textured samples.

Increasing firing temperature increases contact recombination in all cases. The FT contacts on the thickest polySi layers generate contact recombination of only around 100-200 fA/cm^2. The $J_{o,c}$ of FT contacts on n-polySi is observed to be more sensitive to layer thickness than on p-polySi, and a $J_{o,c}$ value of 1400 fA/cm^2 is reached for nominal thickness of 75 nm n-polySi fired at 825°C, compared to around 400 fA/cm^2 for the equivalent p-polySi sample.

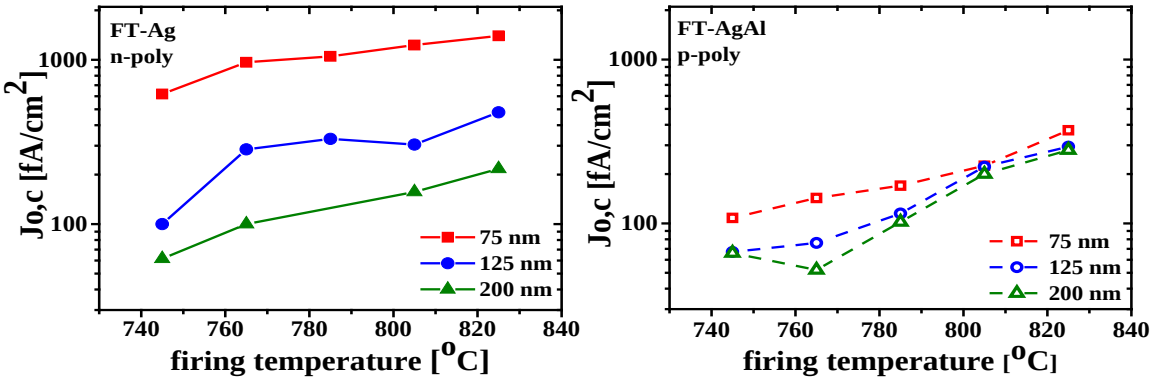

Fig. 5. Modelled $J_{o,c}$ for FT Ag paste on n-poly/wafer/n-poly (left) and FT AgAl paste on p-poly/wafer/p-poly (right) for 75, 125 and 200 nm poly layers fired at five different firing temperatures.

3.4. Extraction of $J_{o,c}$ from V_{oc} measurements

Metallization of all-polySi cells (cf. Fig. 2c) with FT paste resulted in a voltage loss of 30-40 mV relative to the iV_{oc} of the unmetallized half-fabricate, for both polished and textured cells. With NFT paste the observed voltage loss was around 20 mV. Results are summarized in Table 2. There is no clear advantage in V_{oc} for the thicker polySi compared to the thinner polySi. With the J_o values from the previous section, for the FT paste a reduction in V_{oc} of about 14 mV (200 nm) and 33 mV (100 nm) would have been expected, respectively.

Table 2. Measured best and average iV_{oc} *(mV)* and total $J_{o,pas}$ *(fA/cm²)* for all-polySi half-fabricates, and the corresponding V_{oc} *(mV)* and FF (%) of best cells obtained with FT and NFT metallization for 100 and 200 nm thick polySi layers.

thick.	*polished*								*textured*							
	SiN_x as depo.		SiN_x + firing		FT+firing 785°C		NFT+curing		SiN_x as depo.		SiN_x + firing		FT+firing 785°C		NFT+curing	
	iV_{oc}	J_o	iV_{oc}	J_o	iV_{oc}	FF	iV_{oc}	FF	iV_{oc}	J_o	iV_{oc}	J_o	iV_{oc}	FF	iV_{oc}	FF
100	721 705±17	19 47±34	729 715±15	11 30±21	700	37	709	76.2	702 699±2	46 51±3	712 709±2	30 33±3	666	73	681	73.1
200	712 701±8	29 39±8	727 722±6	12 16±4	691	51	706	69.4	694 689±4	60 66±7	708 704±4	35 39±5	676	73	681	73.1

For further characterization of the contact recombination and comparison with the PL method, test cell patterns, as shown in Fig. 1b, with varying metal contact fractions were processed to quantify separately front and rear contact recombination. Measured V_{oc} values are translated into $J_{o,total}$ using the diode equation eq. (2).

$$V_{oc} = \frac{kT}{q} ln\left(\frac{J_{sc}}{J_{o,total}} + 1\right) \quad (2)$$

Then, $J_{o,c}$ is extracted from the slope of $J_{o,total}$ vs. metal area fraction, as shown in Fig. 6. Although the minimum finger area fraction was 2%, the two busbars per cell contribute 6.5% metal coverage, resulting in a minimum total metal fraction of 8.5%, increasing up to 38.5%. The busbars consisted of the same FT paste as the fingers, and it is well known that busbar area contributes to recombination and V_{oc} loss due to metallization. However, the calculation of metal area fraction of the cell, where each cell area is defined as being delimited by the two busbars and the two outer fingers (see Fig. 1b) is somewhat arbitrary. For this reason, Fig. 6 only shows the results with finger metallization fraction of at least 8%, i.e total metal fraction larger than 14.5%. As seen in Fig. 6 (left), $J_{o,total}$ has a large standard deviation for the J_o-test pattern on the 100 nm thick poly layers, in particular the n-polySi layers. This could be related

to the thinning of the n-poly layer during glass removal after diffusion, which could make the $J_{o,contact}$ on the thinnest n-poly very sensitive to small fluctuations in processing, e.g., firing temperature.

n-poly / Ag paste	thick. (nm)	Jo,c (fA/cm^2)
	100	1084±461
	200	386±22

p-poly / AgAl paste	thick. (nm)	Jo,c (fA/cm^2)
	100	796±103
	200	319±40

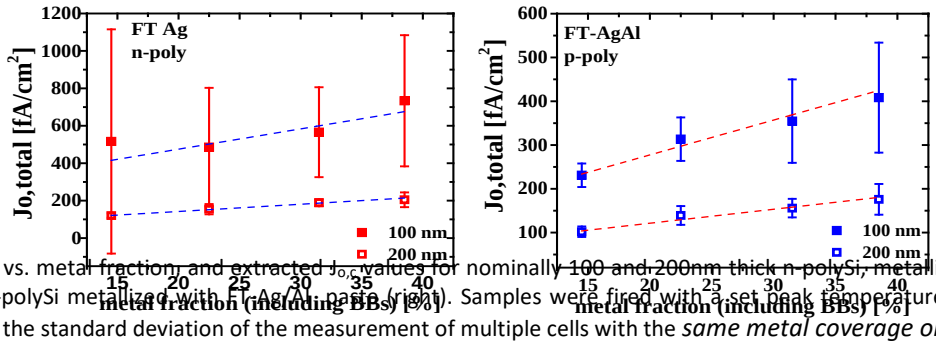

Fig. 6. $J_{o,total}$ vs. metal fraction and extracted $J_{o,c}$ values for nominally 100 and 200nm thick n-polySi, metallized with FT-Ag paste (left) and p-polySi metallized with FT-Ag/Al paste (right). Samples were fired with a set peak temperature of 825°C. The error margins are the standard deviation of the measurement of multiple cells with the *same metal coverage on one wafer.*

3.5. Comparison of $J_{o,c}$ obtained with different methods

The $J_{o,c}$ values from PL modelling of 1400, 480 and 220 fA/cm^2 for respective n-polySi thicknesses of 75, 125 and 200 nm fired with the peak temperature of 825°C, are comparable to the $J_{o,c}$ values of 1084±461 (for 100 nm) and 386±22 fA/cm^2 (for 200 nm) obtained from the V_{oc} measurements. The obtained $J_{o,c}$ values are somewhat higher than in earlier tests with n-polySi back contact on the PERPoly cells, where the contact recombination was estimated to be in the range of 100-200 fA/cm^2 for 200 nm n-polySi [3].

The V_{oc} measured for the nominally 100 nm thick p-polySi layers was observed to be less scattered compared to 100 nm thick n-poly layers, which could be related to the greater layer thickness, or less aggressiveness of the AgAl FT-paste. Less detrimental contacting of Ag/Al paste on p-polySi is also confirmed by the PL modelling results of $J_{o,c}$ of 400 and 250 fA/cm^2 for respective nominal thicknesses of 75 and 200 nm, compared to 796±103 and 319±40 fA/cm^2 from V_{oc} measurements.

Using the $J_{o,c}$ values obtained from the test structure analysis, the V_{oc} of full area all-polySi cells metallized with H-patterns on both surfaces was calculated to be 670±11 mV (100 nm polySi thickness) and 690±4 mV (200 nm polySi thickness). In contrast, the actual cell V_{oc} values were 666 mV and 676 mV for 100 and 200 nm polySi, respectively.

3.6. HR-SEM imaging of FT contacts on polySi

A detailed SEM study was carried out on the previously described samples with 100 nm polySi on textured wafers, metallized with FT paste and fired at 785 and 825°C. Fig. 7 shows images of samples that were processed first with aqua regia to remove the bulk of the metal paste, and subsequently with HF to remove the glass frit, leaving only the metal close to the wafer surface that was initially covered with glass frit. Fig. 7 additionally shows images of samples that were subsequently again processed with aqua regia to remove the final agglomerates of metal paste, showing the damage and pits resulting from intrusions of the paste into the wafer surface.

On sample cross sections of the n-polySi metallized with Ag FT paste, firstly it is striking that on large surface areas the polySi layer appears to have been completely removed by the metallization paste, while in other areas it remained largely intact. For example, in Fig. 7 (b) no remaining polySi layer is visible, whereas Fig. 7(c) shows a transition between polySi-covered and bare areas. Metal intrusions into the c-Si wafer surface where the polySi layer was completely removed were observed for both 785 and 825°C as seen in Fig. 7(a) and Fig. 7(d) respectively. Presence of metal in these intrusions was confirmed by back scattered electron (BSE) imaging. Applying aqua regia after HF etching made the damage on n-polySi better visible. Pits of ~100 nm diameter, distributed all over the polySi-free wafer surface, are observed in Fig. 7(b).

Lowering the firing temperature from 825°C to 785°C does not reduce the damage significantly: Ag agglomerates intrusion into the wafer and local removal of the n-polySi layer, are already present after firing at 785°C. SEM images of two samples fired at 785 and 825°C taken with the same microscope settings were processed and analysed for pit area. Analysis showed that reducing firing temperature from 825 to 785°C reduces pit area from 4.9 to 3.6% with corresponding $J_{o,c}$ drop from 480 to 330 fA/cm^2 shown in Fig. 5(left).

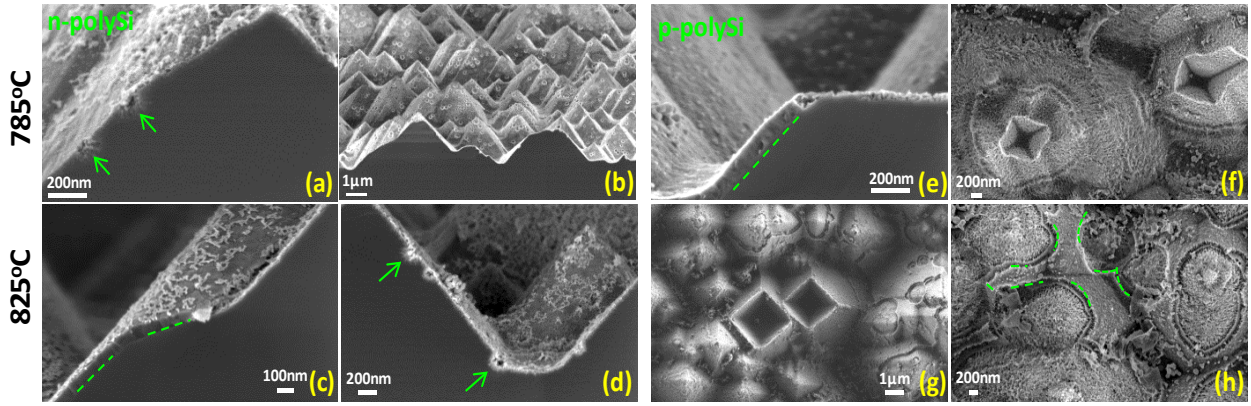

Fig. 7. High Resolution SEM investigation of polySi interaction with fire through pastes on textured surfaces. The samples have been processed first with aqua regia to remove the bulk of the metal paste, and subsequently with HF to remove the glass frit, leaving only the metal close to the wafer surface that was covered with glass frit (Fig. a,c,d,e). Subsequent further etching with aqua regia removed the last metal (Fig. b,f-h). The green dashed lines indicate the boundary polySi/wafer. Green arrows point at metal intrusions into the wafer.

As shown in Fig. 7(e), cross-section analysis of the p-poly side of the same samples after glass removal revealed that local removal of the polySi layer also happens for p-polySi, even after firing at the lowest temperature (785°C). The p-polySi layer is typically removed from the texture pyramid tips, whereas it is often still present intact in the valleys between the texture pyramids. Top-view analysis also showed the existence of large pits with inverted pyramid shape with (111) facets at the tips of some texture pyramids (Fig. 7(f)), indicating that Si is replaced by metal that grows into Si [11]. Removing remaining Ag/Al particle agglomerates using aqua regia visualizes the extent of damage to the polySi layer and the underlying c-Si surface. Fig. 7(h) shows that where the polySi layer is removed the underlying c-Si surface is damaged. Increasing the firing temperature from 785 to 825°C promotes the formation of the inverted pyramids at the tips of texture pyramids, as seen in Fig. 7(g). This coincides with reduced ρ_{co} as observed in Fig. 3 (right) and increased recombination losses in Fig. 6. The recombination losses of p-polySi contacted with FT-Ag/Al paste increase as a function of increasing firing temperature with only a slight dependence on layer thickness.

3.7. HR-SEM imaging of NFT contacts on polySi

All-polySi cells metallized with NFT paste on polished wafers were analysed by SEM following the removal of bulk metal using aqua regia. Small openings and locally thinned regions were observed on both n-poly and p-poly side of the samples as seen in Fig. 8. Unlike FT paste, no extensive etching of poly layer was observed for NFT paste other than small shallow openings. This should be favorable for a passivating contact structure.

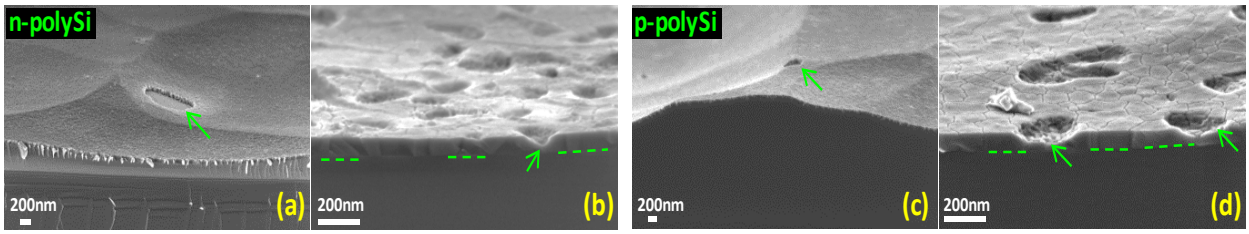

Fig. 8. High Resolution SEM investigation of polySi interaction with non-fire through pastes on polished surfaces. The green dashed lines indicate the boundary polySi/wafer. Green arrows point local damages on polySi layer.

The gentler contacting mechanism of NFT paste was expected to suppress contact recombination losses. However, samples metallized with NFT paste still show a significant V_{oc}-loss at cell level as shown in Table 2. Possible explanations include hydrogen effusion during curing of the paste (patterning of SiNx prior to printing created wider openings than printed finger width), or a detrimental metal-polySi interaction. However, curing of samples with patterned SiN_x but without NFT paste did not show any degradation. Therefore, the degradation is more likely affected by some kind of local damage to the polySi layer or metal-polySi interaction.

3.8. Contact formation of FT paste on polySi

The SEM images suggest that contact formation of FT-Ag paste on n-polySi layers is based on either i) Ag nanoparticle agglomerates on the remaining areas of n-polySi layer, or ii) intrusions of Ag into the wafer where the n-polySi layer has disappeared. Given the removal of large areas of n-polySi layer the relatively low $J_{o,c}$ is perhaps surprising, and suggests some passivation from frit and/or an effect of surface doping from the phosphorus in the dissolved n-poly. To understand the contact and passivation mechanism better, SEM characterisation as presented should be conducted for increased polySi layer thickness

The SEM images suggest that contacting of FT-AgAl on p-poly is by either i) the large inverted pyramids, ii) Ag nanoparticle agglomerates on the wafer where the p-polySi layer was removed, or iii) Ag nanoparticle agglomerates on the p-polySi layer where it was not removed. Considering the very high ρ_{co} values of p-polySi measured on polished wafers, it is likely that i) is the main mechanism for the contacting of p-polySi layers. In Fig. 7(f, g) increasing firing temperature was observed to increase the depth and width of the inverted pyramids, which is consistent with improved ρ_{co} as a function of increasing firing temperature shown in Fig. 3(right). Since these inverted pyramids penetrate several microns deep into the underlying Si wafer [13], there is no thickness dependence of ρ_{co}. These inverted pyramids do not shunt the emitter, which probably is as a result of high acceptor concentration at the interface with the wafer [15]. Their area coverage is only about 1% [16] of the metallized region which is enough to form a proper contact and which results in lower $J_{o,c}$ compared to the Ag paste on n-polySi layers. Also, a large fraction of the rest of the surface under the printed metal contact is still passivated by the remaining p-polySi layer.

4. Conclusions

We presented studies of both p-type and n-type polysilicon passivating contacts and their metallization with industrial fire through (FT) screen printed pastes. The carrier selective polySi/SiO_x passivating contact layers were produced with an LPCVD based polySi deposition process on both sides of 6 inch Cz wafers. The polySi/SiO_x passivating layers, with thickness down to 50 nm, resulted in very low J_o. The FT metal contacted polySi was analysed in terms of contact resistivity, contact recombination and resulting cell performance, for different polySi thicknesses, and pastes fired at various temperatures. Contact recombination was analysed both by using a newly-developed modelling procedure based on QSSPC-calibrated PL measurements, and by means of V_{oc} measurements for various metal fractions. Results from both methods were in approximate agreement, with $J_{o,c}$ around 400 (1400) and 350 (800) fA/cm^2 for n-polySi and p-polySi layers of 200 (100) nm thickness. HR-SEM imaging of contacted regions strikingly revealed that the FT-metallization locally removed large fractions of the polySi layer, and damaged the underlying substrate, by means of mainly Ag intrusions on the n-polySi contacted with industrial Ag paste, and Al-

based inverted pyramids on the p-polySi contacted with industrial AgAl paste. The SEM images combined with other results also hinted at possible mechanisms and pathways for the electronic contact. The Al-based inverted pyramids are likely the main contributor for the contacting of p-polySi layers. Considering that conventional FT metallization on high performance (low doped) homojunctions results in $J_{o,c}$ of about 2500 fA/cm^2 [17], the $J_{o,c}$ determined on the polySi layers of 200 nm thickness is already an order of magnitude lower, with resulting significant benefit for cell V_{oc}. To have full benefit of the excellent low J_o of the non-contacted polySi areas, further work needs to be done to strongly reduce $J_{o,c}$ of FT metallization in particular for the thinnest polySi layers. A companion paper at this conference reports recent progress on FT contacting on n-polySi [5] showing that very low $J_{o,c}$ can be achieved also on 100 nm thick polySi.

Acknowledgments

Part of this work was performed in the project NexPas (TEZ0214002), which receives funding from the Topsector Energie of the Dutch Ministry of Economic Affairs.
Mark Smithers[c] is gratefully acknowledged for HR-SEM imaging.

References

[1] P. Stradins, A. Rohatgi, S. Glunz, J. Benick, F. Feldmann, S. Essig, W. Nemeth, A. Upadhyaya, B. Rounsaville, Y.-W. Ok, B. Lee, D. Young, A. Norman, Y. Liu, J.-W. Luo, E. Warren, A. Dameron, V. LaSalvia, M. Page and M. Hermle, “Passivated tunneling contacts to n-type wafer silicon and their implementation into high performance solar cells,” in WCPEC-6: 6th World Conference on Photovoltaic Energy Conversion, Kyoto, Japan, 2014.
[2] F. Feldmann, M. Bivour, C. Reichel, M. Hermle and S. W. Glunz, “Passivated rear contacts for high-efficiency n-type Si solar cells providing high interface passivation quality and excellent transport characteristics,” Solar Energy Materials and Solar Cells, no. 120, pp. 270-274, 2014.
[3] E. Yablonovitch, R. M. Swanson and Y. H. Kwark, in Proceedings of the 17th IEEE Photovoltaic/Spec. Conf., 1984.
[4] M. Stodolny, M. Lenes, Y. Wu, G. Janssen, I. Romijn and J. Luchies, "n-Type polysilicon passivating contact for industrial bifacial n-type solar cells," Solar Energy Materials and Solar Cells, no. 158, pp. 24-28, 2016.
[5] M. Stodolny, L. Geerligs, G. Janssen, B. van de Loo, J. Melskens, R. Santbergen, O. Isabella, J. Schmitz, M. Lenes, J. Luchies and W. Kessels, “Material properties of LPCVD Processed n-type Polysilicon Passivating Contacts and Application in PERPoly Industrial Bifacial Solar Cells,” in Energy Procedia, Freiburg, Germany, 2017.
[6] B. Thuilier, J. Boyeaux, A. Kaminski and A. Laugier, “Transmission electron microscopy and EDS analysis of screen-printed contacts formation on multicrystalline silicon solar cells,” Materials Science and Engineering:B, vol. 102, no. 1-3, pp. 58-62, 2003.
[7] D. Kane and R. Swanson , “Measurement of the emitter saturation current by a contactless photoconductivity decay method,” in 18th IEEE Photovoltaic Specialists Conference, Las Vegas: 1985. p. 578..
[8] S. Eidelloth and R. Brendel, “Analytical Theory for Extracting Specific Contact Resistances of Thick Samples From the Transmission Line Method,” IEEE ELECTRON DEVICE LETTERS, vol. 35, no. 1, pp. 9-11, 2014.
[9] A. Fell, “A Free and Fast Three-Dimensional/Two-Dimensional Solar Cell Simulator Featuring Conductive Boundary and Quasi-Neutrality Approximations,” IEEE TRANSACTIONS ON ELECTRON DEVICES, vol. 60, no. 2, pp. 733-738, 2013.
[10] A. Fell, K. McIntosh, M. Abbott and D. Walter, “Quokka version 2: selective surface doping, luminescence modeling and data fitting,” in 23rd Photovoltaic Science and Engineering Conference (PVSEC), Taipei, 2013.
[11] J. Deckers, X. Loozen, N. Posthuma, B. O'Sullivan, M. Debucquoy, S. Singh, M. Aleman, M. Payo, I. Gordon, P. Verlinden, R. Mertens and J. Poortmans, “Injection dependent emitter saturation current density measurement under metallized areas using photoconductance decay,” in 28th European Photovoltaic Solar Energy Conference and Exhibition, 2013.
[12] S. Fritz, M. König, S. Riegel, A. Herguth, M. Hörteis and G. Hahn, “Formation of Ag/Al Screen Printing Contacts on B Emitters,” IEEE Journal of Photovoltaics, vol. 5, no. 1, pp. 145-151, 2015.
[13] S. Fritz, S. Riegel, A. Herguth and G. Hahn, “Influence of Si surface orientation on screen-printed Ag/Al contacts,” in 5th International Conference on Silicon Photovoltaics, SiliconPV 2015, Konstanz, Germany, 2015.

[14] W. Wu, K. E. Roelofs, S. Subramoney, K. Lloyd and L. Zhang, “Role of aluminum in silver paste contact to boron-doped silicon emitters,” AIP Advances, vol. 7, no. 015306, 2017.
[15] S. Riegel, F. Mutter, T. Lauermann, B. Terheiden and G. Hahn, “Review on screen printed metallization on p-type silicon,” in 3rd Workshop on Metallization for Crystalline Silicon Solar Cells: Energy Procedia, Charleroi, Belgium, 25-26 October, 2011.
[16] N. Wöhrle, E. Lohmüller, S. Werner and J. Greulich, “Development, Characterization and Modelling of Doping Profile, Contact Resistance and Metal Spiking in Diffused and Screen-Printed Boron Emitters,” in 31st European PV Solar Energy Conference and Exhibition, Hamburg, Germany, 14-18 September, 2015.
[17] B. Geerligs, M. Stodolny, Y. Wu, A. Gutjahr, G. Janssen, I. Romijn, J. Anker, E. Bende, H. Ciftpinar, M. Lenes and J. M. Luchies, “LPCVD polysilicon passivating contacts,” in Workshop on Crystalline Silicon Solar Cells and Modules: Materials and Processes, Vail, Co., USA, 28 - 31 August 2016.
[18] E. Cabrera, S. Olibet, J. Glatz-Reichenbach, R. Kopecek, D. Reinke and G. Schubert, “Current transport in thick film Ag metallization: Direct contacts at Silicon pyramid tips?,” in Energy Procedia, Freiburg, Germany, 2011.
[19] S. Sze, Semiconductor Devices: Physics and Technology, John Wiley & Sons Inc., 1998.
[20] E. Cabrera, S. Olibet, D. Rudolph, P. E. Vullum, R. Kopecek, D. Reinke, C. Herzog, D. Schwaderer and G. Schubert, “Impact of excess phosphorus doping and Si crystalline defects on Ag crystallite nucleation and growth in silver screen-printed Si solar cells,” Progress in Photovoltaics: Research and Applications, vol. 23, pp. 367-375, 2015.
[21] D. Meier, E. Good, R. Garcia, B. Bingham, S. Yamanaka, V. Chandrasekaran and C. Bucher, “DETERMINING COMPONENTS OF SERIES RESISTANCE FROM MEASUREMENTS ON A FINISHED CELL,” in IEEE 4th World Conference on Photovoltaic Energy Conference, Waikoloa HI, USA, 2006.

Beschrijving van de bijdrage van het project aan de doelstellingen van de regeling (duurzame energiehuishouding, versterking van de kennispositie)

De projectpartners hebben op het gebied van apparatuur, processing en eigenschappen van selectieve contacten op basis van gedoteerd polysilicon veel nieuwe kennis opgedaan. Deze kennis wordt al gebruikt voor het op de markt zetten van deze nieuwe technologie. De technologie heeft potentie voor toepassing in veel verschillende zonnecelconcepten, en er is daarom zeer veel interesse van de zonnecelproducerende industrie. Daarnaast hebben de partners aangetoond hoe n-type polySi specifiek in een n-PERT (n-Pasha) zonnecelproces kan worden toegepast, ook in industriële productielijnen, waarmee op goedkope wijze significante verbetering van rendement (tot 22% of meer) bereikt kan worden. In het project is een celrendement tot 20.7% gerealiseerd. In vervolgontwikkeling op basis van dezelfde processen is inmiddels een zonnecelrendement van 21.5% gerealiseerd. Deze rendementen zijn behaald met cellen van standaard industriële grootte en met processen die toepasbaar en opschaalbaar zijn tot industriële productie van grote volumes. Het onderzoek en de ontwikkeling van dit n-PERT concept met n-polySi, alsmede andere celconcepten met polySi, vond en vindt nu plaats in andere TKI projecten. Er is bovendien een basis gelegd voor IBC (achterzijde contact) cellen met selectieve contacten van gedoteerd polysilicon, waarvoor ook verdere ontwikkeling plaatsvindt in andere TKI projecten.

Spin off binnen en buiten de sector

Binnen de PV sector kan de technologische bijdrage deels gemeten worden aan de hoeveelheid publicaties en conferentiebijdragen die zijn gedaan door de projectpartners. De lijst hiervan is onderaan dit rapport toegevoegd. Daarnaast staat polySi sinds 2014 enorm in de internationale belangstelling, en de resultaten die vanuit dit project zijn gepubliceerd, en die zeer goed aansluiten bij de industriële processen, hebben daar zeker aan gedragen.

Verschillende celfabrikanten hebben aangegeven, bij Tempress en bij ECN, belangstelling te hebben voor de processen en celconcepten die zijn ontwikkeld in het project.

De kennis opgedaan in het project op het gebied van polySi zou ook voor een deel interessant kunnen zijn voor andere toepassingsgebieden, bijv. in ander halfgeleiderondersoek (zowel voor IC industrie als laag-TRL onderzoek), waarmee al een link is vanuit het marktgebied van Tempress, en het onderzoeksgebied van UT.

Overzicht van openbare publicaties over het project en waar deze te vinden of te verkrijgen zijn

Publicaties and presentaties van het project:

Auteurs (partner)	Titel	Gelegenheid/Tijdschrift, Datum
M. Lenes et al. (Tempress) and M. Stodolny et al. (ECN)	LPCVD doped poly passivated contacts for Si-cell technology	Presentation at Asia PV conference, 29-10-2015
M. Stodolny et al. (ECN) and M. Lenes et al. (Tempress)	n-Type polysilicon passivating contact for industrial bifacial n-type solar cells	Solar Energy Materials & Solar Cells 158, pp. 24-28 (2016). Also presentation at 6th International Conference on Silicon Photovoltaics, SiliconPV 2016.
B. Geerligs et al. (ECN) and M. Lenes et al. (Tempress)	LPCVD polysilicon passivating contacts for crystalline silicon solar cells	Photovoltaics International Magazine, Volume 32 (May 2016), pp. 43-52.
M. Stodolny et al. (ECN) and M. Lenes et al. (Tempress)	n-Type polysilicon passivating contact for industrial bifacial n-type solar cells	Presentation, and proceedings of the 32nd European PVSEC, June 20-24, 2016, Munich, Germany, pp. 460-465
L.J. Geerligs et al. (ECN) and M. Lenes et al. (Tempress)	LPCVD polysilicon passivating contacts	Invited presentation and article contribution to workshop handout, Workshop on Crystalline Silicon Solar Cells and Modules: Materials and Processes, Vail, Co. August 28-31, 2016.
H.E. Ciftpinar et al. (ECN, Tempress, UTwente)	Study of screen printed metallization for polysilicon based passivating contacts	Energy Procedia 124 (2017) 851–861. Also presentation at 7th International Conference on Silicon Photovoltaics, SiliconPV 2017.
M. Stodolny et al. (ECN, Tempress)	Contact recombination of polysilicon passivating contact with fire-through screen-printed metallization	Presentation at 7th Workshop on Metallization & Interconnection for Crystalline Silicon Solar Cells, 23-24 October 2017, Konstanz, Germany

Alle publicaties zijn te verkrijgen bij ondergenoemde contacten, en in veel gevallen ook te verkrijgen op https://www.ecn.nl/publicaties/.

Overige publicaties die resultaten van het project bevatten:

Auteurs (partner)	Titel	Gelegenheid/Tijdschrift, Datum
ECN	Dutch innovation makes solar cells more profitable	News release on ECN website, 8-3-2016: https://www.ecn.nl/ news/item/dutch-innovation-makes-solar-cells-more-profitable/
J.M. Luchies et al. (Tempress)	Next steps for mass production of low-cost n-type	PV-tech conference, Kuala Lumpur, March 17th, 2016
E. Bende (ECN)	Application of polysilicon passivation in industrial solar cells	Presentation at workshop 'Incremental technology steps for the next generation solar cells and modules' within the 12th Chinese CSPV conference, Shanghai, 25-11-2016
I. Romijn (ECN)	From lab to fab: track record, strategy, and new concepts	Invited presentation at PV CellTech, March 16-17, 2016, Kuala Lumpur, Malaysia
M. Lenes et al. (Tempress)	LPCVD polysilicon passivated contacts for different solar cell concepts	SNEC Conference, 24 May 2016, Shanghai
L.J. Geerligs et al. (ECN) and M. Lenes et al. (Tempress)	Op zoek naar contacten voor zonnecellen	article in Nederlands Tijdschrift voor Natuurkunde (Magazine of the Dutch Physics Society), February 2017
Bas van Aken and Ingrid Romijn (ECN)	Article on bifacial and PERPoly technology (in Chinese)	PES (power & energy solutions), special issue for SNEC PV power expo, 19-21 April 2017, Shanghai
G. Coletti	Polysilicon passivating contacts for n-PERT devices and future technology development	Invited presentation, Workshop on Crystalline Silicon Solar Cells and Modules: Materials and Processes, , Co. August 1, 2017.
M. Stodolny et al. (ECN, Tempress, UTwente, TUDelft, TU-Eindhoven)	Material properties of LPCVD Processed n-type Poly-Si Passivating Contacts and Application in PERPoly Industrial Bifacial Solar Cells	Presentation, and proceedings of the 33rd European PVSEC, 2017, Amsterdam, Netherlands, only presentation is published (no page numbers)
G.J.M. Janssen et al. (ECN)	THE ROLE OF THE OXIDE IN THE CARRIER SELECTIVITY OF METAL/POLY-SI/OXIDE CONTACTS	Presentation, and proceedings of the 33rd European PVSEC, 2017, Amsterdam,

	TO SILICON WAFERS	Netherlands, pp. 256-261
Dengyuan Song (Yingli)	Panda-TOPCon development (in Chinese)	Forum on PV part of the 15th Chinese State Programme, , December 1, 2017.

Alle publicaties zijn te verkrijgen bij ondergenoemd contacten, en in veel gevallen ook te verkrijgen via https://www.ecn.nl/publicaties/.

Meer exemplaren van dit rapport

Meer exemplaren van dit rapport kunnen digitaal worden verkregen via het hieronder genoemde eerste contact.

Contact voor meer informatie

Meer informatie over dit project kan verkregen worden via:
Jan-Marc Luchies, Tempress Systems B.V., e-mail: jmluchies@tempress.nl
L.J. Geerligs, ECN Solar Energy, e-mail: geerligs@ecn.nl.
Jurriaan Schmitz, e-mail: j.schmitz@utwente.nl

Subsidie

Het project is uitgevoerd met subsidie van het Ministerie van Economische Zaken, Nationale regelingen EZ-subsidies, Topsector Energie uitgevoerd door Rijksdienst voor Ondernemend Nederland.